University of Zurich[UZH]

Department of Geography

Differences in Phenology in the Swiss National Park over 5 Years

GEO 511 Master's Thesis

Katharina Böhler

08-742-140

Date of Submission 29.04.2016

Supervised by Dr. sc. nat. Mathias Kneubühler

Faculty representative Prof. Dr. sc. nat. Michael E. Schaepman

Department of Geography, University of Zurich

Acknowledgments

I am grateful for the support and patience of a number of people contributing to the success of my Master's Thesis. First and most important of all, I would like to thank my husband and my sons for their patience and understanding during my studies and especially while working on my Master's Thesis. I additionally want to thank my whole family for supporting me during the last years, which were full of privation and sometimes stressful. I always knew that I could count on your support.

Thanks go to various people at the RSL: Mathias Kneubühler for having time to explain and answer my questions; Michael E. Schaepman for the possibility to write the thesis at the RSL, Andy Hüni and Hendrik Wulf for processing the APEX IS data, and Moritz Bruggisser for joyful distraction while talking about cooking and eating.

Special thanks go to Benjamin Kellenberger, Jörg Weyermann, Jonas Böhler, Fiona Utzinger, Martina Flick and Samuel Witzig for their linguistic and formal support.

Abstract

Remote sensing is an important tool to monitor phenology. In this Master's Thesis differences in phenology in the Swiss National Park (SNP) in Val Trupchun from 2010 to 2015 are analyzed. The purpose was to find a relationship between meteorological data and alpine phenology by using vegetation indices (VI). The start of phenological season (SOPS) was defined as first day with a temperature above $5°C$, called growing degree day 5 (GDD5). For all investigated years, the meteorological data were aggregate to day of year (DOY) 175, the earliest Airborne Prism EXperiment Imaging Spectrometer (APEX IS) acquisition date in 2010. In this data set, test sites in forest and grassland vegetation classes were selected and suites of relevant VIs were calculated. Correlations of VIs and meteorological data were found for Normalized Differential Vegetation Index (NDVI), Soil Adjusted Vegetation Index (SAVI), Modified Soil Adjusted Vegetation Index 2 (MSAVI2) and Simple Ratio (SR). In particular, very strong correlations between VIs of forest and days with precipitation as well as between VIs of grassland and the total amount of precipitation were found. Further, the Normalized Difference Water Index (NDWI) and Normalized Canopy Index (NCI) showed inconsistent correlations with meteorological data. There were no correlations of VIs and temperature, GDD5, global radiation and sunshine duration. Calculated differences between vegetation subclasses were found on a yearly base but not over all years. The calculation of correlations between subclasses to meteorological data was not possible due to missing specific meteorological data for each test site. In the study area of Val Trupchun, the main constraint is precipitation, in contrast to temperature postulated by other researchers for high alpine regions. Further research on meteorological impact on high alpine vegetation phenology by using VIs is desirable.

Contents

List of Figures

List of Tables

1. Introduction

Alpine vegetation systems are highly vulnerable to climate (Beniston and Rebetez, 1996; Theurillat and Guisan, 2001), and the responses of phenology to climate therefore of particular interest (Busetto et al., 2010). In addition, climatic variables are often used in combination with other environmental factors to explain main vegetation patterns around the world (Guisan and Zimmermann, 2000). Vegetation patterns can be related to physical limits that are caused by environmental and physiological constraints (Guisan and Zimmermann, 2000) also known as gradients (Austin, 1980). The literature differentiates between direct gradients (e.g. air temperature, soil pH), which are not consumed by plants, indirect gradients (e.g. slope, aspect, elevation) with no direct physiological relevance and resource gradients (e.g. nutrients, water, light), which are consumed by plants (Austin, 1980). These gradients are conventionally summarized into most important constraints like temperature, water availability and radiation (Nemani et al., 2003).

The introduction is organized into four parts: environmental constraints in high alpine regions, phenology and phenological key drivers, phenology and remote sensing by using vegetation indices, and motivation and associated research questions.

1.1. Environmental Constraints

1.1.1. Temperature

Temperature in high alpine regions is one of the most important limiting factors. This can be explained by the fact that vascular plants growth can only take place at temperatures above the freezing point (Ladinig and Wagner, 2005). Temperature below the freezing point can cause frost dryness due to non-available water caused by frozen soil (Gebhardt et al., 2007). According to the literature, other resources than temperature (like precipitation) are not a limiting factor for productivity in high alpine regions (Schultz and Halpert, 1993; Whittaker and Niering, 1975). Hence, the growth of trees and flowering of plants is mainly temperature dependent (Kudo and Suzuki, 1999; Moser et al., 2010). Nevertheless, a number of studies mention additional constraints having an impact on plant growth, like water availability (Ladinig and Wagner, 2005) or temperature the latter being of particular importance in the early growing season (Wang et al., 2003).

1.1.2. Water Availability

Water availability is one of the most important constraints for plant growth all over the globe (Jolly et al., 2005; Nemani et al., 2003). Water sources available to plants usually comprise precipitation, snowmelt and ground water. Especially in higher alpine regions snowmelt and precipitation are the dominant sources. Studies in the Chinese alpine regions determine precipitation as a primary constraint for alpine grassland and mountain steppe (Sun et al., 2013)). Furthermore, the elevation gradient at higher altitudes influences precipitation directly (Kariyeva and van Leeuwen, 2011) in a way that the probability for precipitation increases with higher altitudes (Whittaker and Niering, 1975).

1.1.3. Solar Radiation

The third main climatic constraint, solar radiation, is the primary driver for photosynthesis. It provides the plants with the energy required for growth. Solar radiation is more intense at higher altitudes (Blumthaler, 2012). It is therefore common to use solar radiation measurements to estimate efficiencies in photosynthesis (Szeicz, 1974).

The three constraints temperature, water availability and solar radiation are not always equally limiting, but they always interact and lead to varying limitations on vegetation activity and phenology over the whole growing season (Nemani et al., 2003).

1.2. Phenology

The International Biological Program (IBP) defines phenology as “the study of the timing of recurrent biological events, the causes of their timing with regard to biotic and abiotic forces, and the interrelation among phases of the same or different species” (Lieth, 1974). The annual course of vegetation development events differs from year to year depending on changes within climatic gradients. Phenology varies not only over geographic gradients but also over climate zones, vegetation types and weather conditions (Richardson et al., 2013). In the nival belt, phenological development takes place within one to three months (Ladinig and Wagner, 2005). According to Richardson et al. (2013), phenology at higher altitudes is typically influenced by two critical factors, namely the last day of snowmelt and the course of the temperature afterwards. In the following section these phenological key drivers will be briefly introduced.

1.2.1. Snowmelt and Frost

Snowmelt and frost events are not a direct climatic factor. Both depend on the depth of the winter snow pack and springtime temperature (Richardson et al., 2013) and influence the flowering phenology (Inouye et al., 2002). Furthermore, snowmelt is a key factor for growth of alpine plants and is understood as start of growing season (Hoye et al., 2007; Ide and Oguma, 2013; Inouye et al., 2002; Kudo and Suzuki, 1999), whereas snow coverage blocks sunlight for photosynthesis, and spends shelter from severe cold and supplies moisture (Ide and Oguma, 2013). Areas with late snowmelt profit from a higher soil moisture content. Water availability is therefore not a constraint (Hoye et al., 2007). In contrast, advanced snowmelt causes a lengthening of the growing season and harsher growing conditions by increasingly exposing in a way that plants to frost damage with early snowmelt (Wipf et al., 2006). On the other hand, a lengthening of the growing season can result in a higher amount of growing degree days (see below) and thus the available heat and energy for plants (Wipf et al., 2006).

1.2.2. Growing Degree Days

The sum of days with temperature above a certain threshold is called Growing Degree Days (GDD) (Ladinig and Wagner, 2005). GDD can be seen as an approximation to heat and energy for plant development (Yang et al., 1997) and heat accumulation during the phenological phase (Ladinig and Wagner, 2005). Hence, GDD models the role of temperature for vegetation (Ladinig and Wagner, 2005). The temperature threshold value can be set individually. A commonly used threshold is $0°C$ (Ladinig and Wagner, 2005), called GDD0, or a threshold of $5°C$ (GDD5) (Leuzinger et al., 2013; Moser et al., 2010; Wipf et al., 2006). Due to its temperature dependency, GDD decreases with higher altitudes.

1.2.3. Altitude

The altitude above sea level (a.s.l.) directly influences temperature and precipitation (Kariyeva and van Leeuwen, 2011). Especially in mountainous landscapes, altitude is one of the most influencing drivers of the variation in vegetation dynamics (Kariyeva and van Leeuwen, 2011). Phenological change in mountainous ecosystems is mediated by altitude because of direct influence on temperature (Chapman, 2013). In addition, the total atmospheric pressure as well as relative concentration of certain life-supporting gases (in particular CO_2 and O_2) decrease at higher altitudes and radiation increases at cloudless sky (Körner, 2007). It is well known that altitude causes an average decrease of temperature of $0.5°C$ per $100m$ (Moser et al., 2010).

Summarizing the previous sections, factors like snowmelt and frost are important drivers for vegetation at higher altitudes. The high altitude directly influences the GDD as the average temperature decreases with elevation causing an elongation of snow cover duration.

Climatic changes like warming of the atmosphere have varying influences on vegetation at higher altitudes (Menzel, 2002). On a global scale, the biggest changes are predicted for snow-dominated regions at higher altitudes. In a study performed in the European alpine region, an earlier flowering of grasses and woody species of 1 to 5 days per decade in the years before 2000 was found (Ziello et al., 2009). These patterns were linked to warming trends in the same period. Furthermore, a forced leaf-out of European larch at a rate of 7 days for each $1°C$ increase in spring air temperature was monitored in the alpine region of Italy (Busetto et al., 2010). Changes in climate are therefore causing observable phenological changes in alpine vegetation.

1.3. Assessment of Phenology Using Remote Sensing

Phenology and phenological changes are an important domain of research in the field of remote sensing (RS). RS provides means of tracking phenological changes by monitoring the reflectance of electromagnetic radiation by vegetation on a temporal basis (Badeck et al., 2004). Phenology of vegetation is measured for example by greenness, leaf area index (LAI), absorption of chlorophyll, green aboveground phytomass, photosynthesis capacity or primary productivity (Lausch et al., 2015). In particular, LAI can be deduced from RS data. The LAI describes the total of one-sided area of green leaves per unit ground area $[m2/m2]$ (Rundquist, 2002; Zhang et al., 2007). LAI varies with vegetation cover from zero (Atacama desert, South America) up to values of eight in Amazonia (Huete et al., 2002).

To detect seasonal patterns of phenology, satellite or airborne remote sensing data can be used (White and Nemani, 2006). VIs are commonly calculated to quantitatively estimate the vitality of vegetation (Bannari et al., 1995; Lillesand et al., 2008). The performance and the suitability of a particular index are generally determined by the sensitivity of the index to a characteristic of interest (Haboudane et al., 2004). The wavelength for vegetation spectra regions in the visual part (VIS, 400 to 700nm) and near infrared region (NIR, 700 to 1300nm) (Lillesand et al., 2008) have been proved to be rich in content (Collins, 1978). In the red part (600 to 700nm), the spectral reflectance of vegetation is characterized by very low values, because most incoming energy is absorbed by plants (Lillesand et al., 2008) (Figure 1.1). The reflectance values increase rapidly in the range of 700 to 740nm. This spectral reflectance pattern of vegetation is generally called "red edge" (Broge & Leblanc, 2001). The difference between red and NIR wavelengths is used for vegetation indices like simple ratio (SR) (Jordan, 1969), normalized difference vegetation index (NDVI) (Rouse et al., 1974), normalized difference water index (NDWI) (Gao, 1996), soil adjusted vegetation index (SAVI) (Huete, 1988) and modified soil adjusted vegetation index (MSAVI2) (Qi et al., 1994). Furthermore, the short wave infrared (SWIR) spectral region (1500-1750nm) contains information on plant water content and is therefore a potential range to detect vegetation presence and status. The normalized canopy index (NCI) (Vescovo and Gianelle, 2008) uses SWIR and green values to calculate grassland phenology.

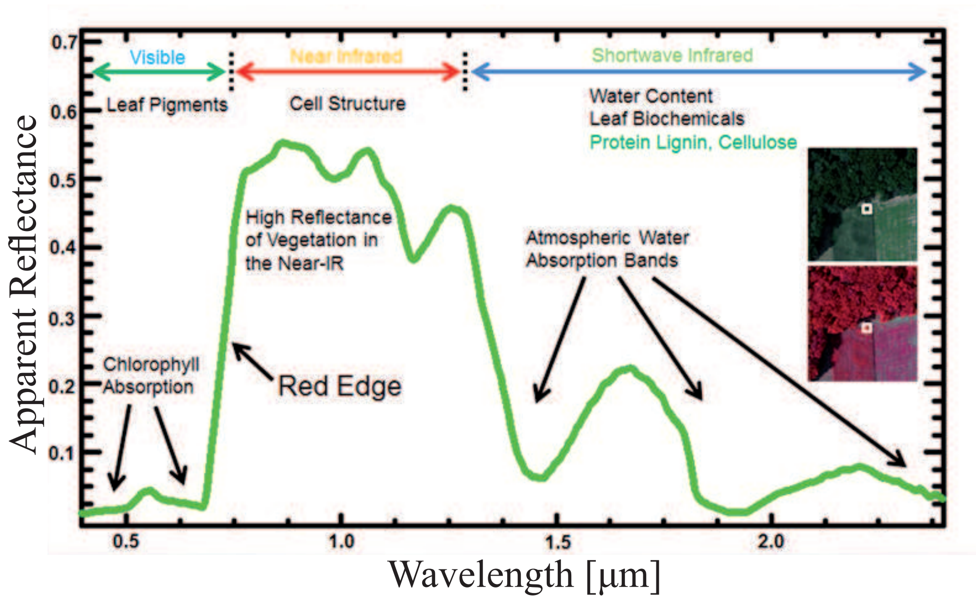

Figure 1.1.: Spectrum of grass with typical spectral features (source: http://www.markelowitz.com/Hyperspectral.html).

The remainder of this section reviews the VIs selected for all further (statistical) analyses.

1.3.1. Simple Ratio (SR)

SR is one of the simplest VIs. SR is usually used in areas with green biomass and was developed for the study of pigment content and pigment concentration (Vescovo and Gianelle, 2008). The benefit of SR is the fact that there is no saturation at high biomass amounts. A disadvantage of SR is its insensitivity to low biomass amounts (Huete et al., 1997). It was demonstrated that SR is a good estimator for biomass in boreal forest (Chen, 1995) and for desert steppe in Inner Mongolia (Ren and Feng, 2014).

1.3.2. Normalized Difference Vegetation Index (NDVI)

The most used VI to monitor phenology in literature is NDVI. It is one of the most used and studied vegetation index to detect biomass and vegetation health because it effectively reflects spatial variations in vegetation (Huete et al., 2002; White et al., 2014, 2009). Furthermore, NDVI is often chosen because it enhances the vegetation signal in low biomass conditions (Broge and Leblanc, 2001; Huete et al., 1997; Liu et al., 2007; Shen et al., 2008). This enhancement in low biomass conditions implies that NDVI shows a saturation effect at higher biomass levels (Huete et al., 1997, 2002; Mutanga and Skidmore, 2004). Nevertheless, NDVI is used as effective indicator of plant dynamics studying the relationship between climatic elements and phenology (Sun et al., 2013). Most of the studies focussing on climatic elements and NDVI investigated the relation between NDVI and precipitation or temperature. There are varying results on NDVI and precipitation. Some studies found a very weak or intermediate correlation of NDVI and precipitation (Mingjun et al., 2007; Yang et al., 1997), others found a strong correlation of NDVI for grassland or forest and precipitation (Hao et al., 2012; Wang et al., 2003). Furthermore, higher temperatures ought to lead to higher NDVI values for vegetation (Braswell et al., 1997; Hao et al., 2012). Seasonal changes in temperature have an additional impact on NDVI scores, with temperature at the beginning and the end of the season being strongly positively related to NDVI (Wang et al., 2003).

1.3.3. Normalized Difference Water Index (NDWI)

The NDWI is a proxy for liquid water in vegetation and is therefore an indicator for vegetation health status (Gao, 1996). NDWI is less sensitive to atmospheric scattering than NDVI but performs worse in regions with low vegetation cover (Gao, 1996). NDWI has not only been reported to show a high potential to monitor phenology in regions with high snowfall and across varying regeneration stages (White et al., 2014) but also correlates with aboveground biomass in alpine grassland studied in Slovakia (Halabuk et al., 2013).

1.3.4. Soil Adjusted Vegetation Index (SAVI)

The SAVI handles soil-background variation which affects the measured vegetation spectra (Haboudane et al., 2004). The SR and NDVI values for vegetation increase with darker soil background (Huete, 1988). A soil adjustment factor is incorporated in SAVI to reduce soil-noise (Qi et al., 1994). SAVI is still sensitive to variations in NIR reflectance (Huete et al., 1997) but less sensitive to chlorophyll. The index is also affected by saturation in dense vegetation cover, however less than NDVI (Haboudane et al., 2004; Shen et al., 2008).

1.3.5. Modified Soil Adjusted Vegetation Index 2 (MSAVI2)

Compared to the conventional SAVI, MSAVI2 additionally adjusts for soil effects in a vegetation signal that varies with the amount of vegetation (Liu et al., 2007; Qi et al., 1994). MSAVI2 is more sensitive to vegetation than SAVI or NDVI (Qi et al., 1994). It seems to be the best estimator for dense canopies (Broge and Leblanc, 2001) because there is no clear saturation at high canopy density (Haboudane et al., 2004). Unfortunately, MSAVI2 is very sensitive to atmospheric effects (Broge and Leblanc, 2001).

Shen et al. (2008) have shown that soil adjusting vegetation indices do not improve estimations of aboveground biomass estimation at high chlorophyll concentration (i.e. dense vegetation), but are useful in estimating aboveground biomass for ecosystems with low or medium vegetation cover such as in the desert steppe of Inner Mongolia.

1.3.6. Normalized Canopy Index (NCI)

NCI was developed to improve greenness or chlorophyll information in remote sensing data. The use of SWIR reflectance enables the inclusion of water content information of the vegetation in the VI. In combination with a green band (500 to$600 nm$) (Lillesand et al., 2008), the production of grassland is reported to become quantifiable (Vescovo and Gianelle, 2008). A strong correlation of NCI and phytomass was not only found for green and dry grass in the Trentino Alps of Italy (Vescovo and Gianelle, 2008), but also for grazed grassland in the Grassland National Park of Canada (Yang et al., 2012). However, a study on rangeland detection in Iran using NCI reports poor accuracy (Barati et al., 2011).

All introduced VIs were eventually developed with a focus on vegetation observation. They show varying saturation levels where they no longer respond to variations in green biomass (Huete et al., 1997). When saturated, the detection of changes in land cover or land use, as well as the retrieval of biophysical vegetation parameters and net primary production from VIs become difficult (Huete et al., 1997). LAI is often used to describe the index saturation. Different VIs saturate at different LAI levels. Indeed, NDVI as well as SR are saturating around a LAI value of three, SAVI around a LAI of four, and for MSAVI2 no clear LAI limitations are reported (Badeck et al., 2004; Haboudane et al., 2004; Lu et al., 2005; Mutanga and Skidmore, 2004).

2. Motivation

The upper part of the Trupchun Valley (Val Trupchun) in the SNP is covered by alpine grasslands, larch and Swiss stone pine forests (Kneubühler et al., 2014). Data acquired on an annual basis using the APEX IS (Schaepman et al., 2015) show visual differences in phenology and snow cover from summer 2010 to 2015 (Figure 2.1). Possible explanations for the differences in vegetation development (phenology) between the years could be varying spatial distributions of snow (Kneubühler et al., 2014) or different weather conditions (Billings and Bliss, 1959; Ladinig and Wagner, 2005; Totland, 1997).

This study provides an in-depth analysis on phenological differences within the years from 2010 to 2015. Different vegetation classes were identified for this purpose. The use of VIs offer the possibility to detect differences between vegetation classes both spatially (i.e. within a single scene) and temporally (between different points in time). The relationship of VI values with environmental constraints and deduced phenological key drivers allows conclusions on the main phenological driver in the higher alpine region of Val Trupchun. Potential correlations of VIs and available meteorological data are investigated by addressing the following research questions:

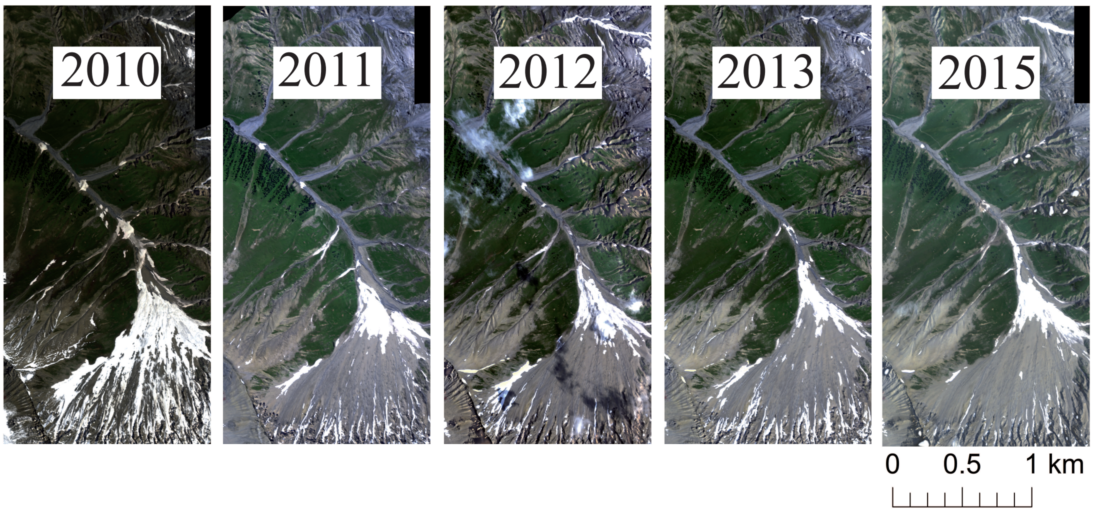

Figure 2.1.: RGB-representation of upper Val Trupchun acquired on 24.06.2010, 26.06.2011, 29.06.2012, 12.07.2013, and 3.07.2015.

2.1. Research Questions

- Are the VIs linearly correlated with temperature?
- Are differences between VI values of vegetation classes linkable to meteorological derivatives and so to environmental constraints and key drivers?
- Are there differences in VI values within vegetation classes due to the fact that there are different terrain aspects?
- Are there differences in VI values between forests with different tree composition depending on environmental constraints and key drivers?
- Are the chosen VIs appropriate to detect differences between vegetation classes in alpine regions?
- Which of the VIs performs best?

3. Material and Methods

3.1. Study Area and Data

3.1.1. Study Area

The SNP is located in the south-western part of Switzerland (Figure 3.1) in the Central Alps and occupies an area of $170 km^2$, ranging in altitude from 1350 to $3170 m a.s.l.$ (Figure 1). Nearly $86 km^2$ are covered with vegetation: roughly $50 km^2$ are covered with forest (mainly pine forest), $33 km^2$ with alpine grassland and $3 km^2$ with subalpine grassland (Schütz et al., 2003). The SNP was founded in 1914 and henceforward all grazing, logging and hunting activities were prohibited (Schütz et al., 2003). The absence of human inventions offers a great possibility to study ecosystem processes like phenological development over years (Kneubühler et al., 2014).

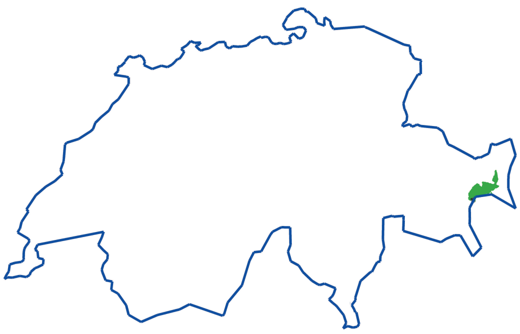

Figure 3.1.: Location of the SNP in the south-east of Switzerland.

The study area of this Master's Thesis is located in the upper part of Val Trupchun in the SNP (Figure 3.2) . Dominant land cover is composed by rocks, bare soil, snow fields, grassland communities and forest (Kneubühler et al., 2014). The south-western exposed hillsides are mainly covered by alpine grassland (1930 to $2570 m a.s.l.$) and small patches of larch and Swiss stone pine forest (Larix decidua Mill. / Pinus cembra L., 1920 to $2160 m a.s.l.$). The north-eastern exposed hillsides are covered by larch and Swiss stone pine forest (1920 to $2240 m a.s.l.$) and grassland (1920 to $2800 m a.s.l.$), accounting to roughly 50% each (Schmid, 2016).

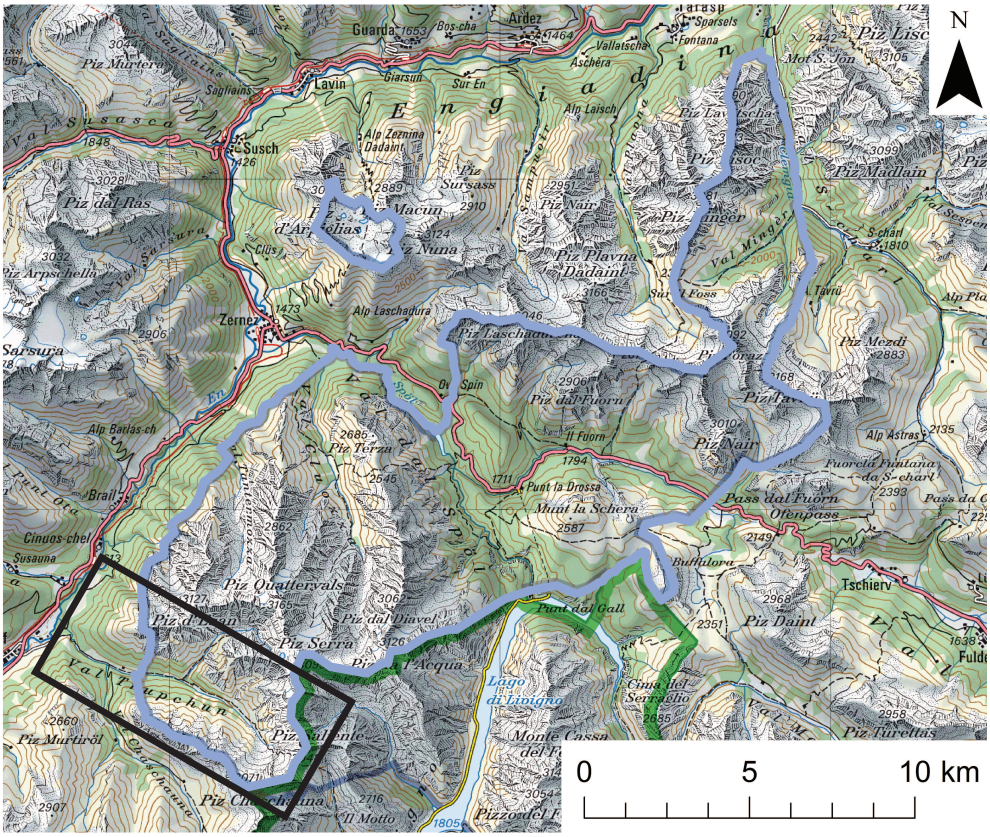

Figure 3.2.: Location of Val Trupchun (black rectangle) in the SNP (light blue boundary). (source background map: Bundesamt für Landestopografie, Switzerland).

3.1.2. Data

3.1.2.1. Airborne Prism EXperiment Imaging Spectrometer (APEX IS) Data

APEX is an airborne pushbroom scanner with 1000 across track pixels covering a field of view of $28 degrees$ (Schaepman et al., 2015). The solar reflected radiation ranging from 0.380 to $2.500 \mu m$ is measured with 334 reconfigurable spectral bands in the visible/near infrared (VNIR) and 198 spectral bands in the SWIR spectral region (Jehle et al., 2010).

APEX IS data sets were acquired over the study site every year from 2010 to 2015 around DOY 175, except for 2014 (Table 3.1). In 2014, data acquisition took place on DOY 270 and was therefore excluded from the data analysis, because it is not comparable phenologically. The flight altitude over the study site ranged between 6600 and $7200 m a.s.l.$, resulting in a resampled pixel size of $2 m$.

The number of flight lines acquired over Val Trupchun varies for the different years. In 2012, unstable meteorological conditions led to a reduced number of acquired flight lines. In 2011, the APEX sensor experienced technical problems and only two flight lines could be acquired. The effective flight lines (sectors) are defined in Table 3.1, the different sectors are presented in Figure 3.3.

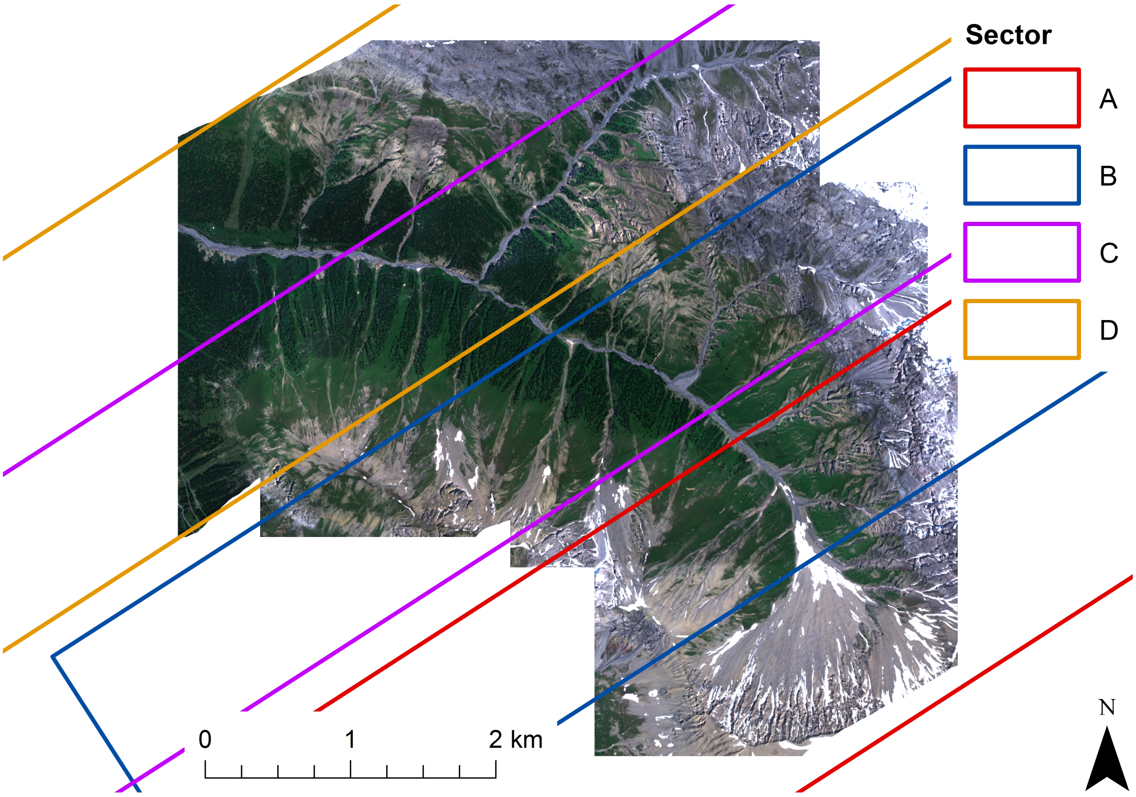

Figure 3.3.: APEX IS acquisition in 2013 of Val Trupchun. The different colored rectangles indicate the four sectors (source sectors: RSL/APEX Flight planning).

3.1.2.2. Digital Elevation Model

The digital elevation model (DEM) used for these thesis has a spatial resolution of $2m$. The accuracy below $2000ma.s.l$ is $+/- 0.50m$, above $2000ma.s.l.$ $+/-1m$ to $3m$ (swissALTI3D, Bundesamt für Landestopografie, Switzerland).

3.1.2.3. Meteorological Data

The closest meteorological station to Val Trupchun is placed at Buffalora (2816494/1170225, CH1903+) at $1968ma.s.l.$, $50m$ outside of the SNP. At Buffalora, mean annual precipitation of $925 \pm 162mm$ and a temperature of $0.2 \pm 0.7°C$ (mean ± SD) were measured between 1904 and 1994 (Risch et al., 2008). Meteorological data for the station Buffalora were obtained from IDAWEB (MeteoSchweiz, 2016).

For this study, meteorological data was collected comprising air temperature measured $2m$ above ground and aggregated to a daily mean (in$°C$), precipitation per day (in mm), global radiation (in W/m^2) and sunshine duration aggregated to a daily sum (in h). It would have been interesting to have data about snow coverage but unfortunately it was not available for every year for the meteorological station in Buffalora. For consistency reasons, no snow coverage data have been used.

Table 3.1.: Dates (DOY) and time (local time) of APEX IS data acquisitions for upper Val Trupchun.

year	DOY	acquisition time		sector
		start	end	
2010	175	11:29	11:56	A, B, C, D
2011	177	14:48	15:15	A, B
2012	180	10:36	11:05	A, B, C
2013	193	11:53	12:20	A, B, B/C, C, D
2015	184	10:35	11:14	A, B, B/C, C

Meteorological Derivatives In this study, SOPS was calculated using GDD5, as mentioned above. The values obtained are recorded in Table 3.2. In 2010, the threshold of $5°C$ was reached for the first time at DOY 114 at Buffalora station. Until DOY 175 (APEX data acquisition date), 33 GDD5 with temperature above $5°C$ were recorded in 2010. For comparability reasons, all meteorological data and derivatives were aggregated to the same ending date (DOY 175). The growing days (GD) between SOPS and the baseline acquisition date (DOY 175) were counted. Temperature (T) was used as summarized value based on GD and GDD5. Global radiation (GR) and sunshine duration (SD) were summarized over GD. The days with precipitation (PD) over the GD period were summarized, as well as the total amount of precipitation (PT).

3.2. Methods

3.2.1. Data Preprocessing

The APEX IS data acquired over the SNP were geometrically and radiometrically corrected, subsetted and subsequently mosaicked as described below. Different vegetation masks were generated and the test sites used in this study were selected.

3.2.1.1. Geometric and Atmospheric Processing

The flight lines of APEX were processed to level L2 (Schaepman et al., 2015) by applying geometrical and radiometrical correction using PARGE (Schläpfer and Richter, 2002) and ATCOR-4 (Richter and Schläpfer, 2002) software packages. The datasets containing the relevant parts of Val Trupchun were geo-rectified using TRAFO (integrated in ATCOR-4) with bilinear interpolation. The chosen coordinate definition is SWISS (CH-1903, Switzerland).

3.2.1.2. Building Subsets and Mosaics

From the available flight lines, subsets of the study site were generated. To get a data set for each year that contains the entire area of the study site the subsets were mosaicked with a feathering of 20 pixels to blend the boundaries of the images. In the year 2012 and 2015, the used subsets contain some clouds. By using the mosaic tool, the less clouded flight line subsets were chosen as top subset. This offered the generation of an optimal mosaic for the respective year. Due to reduced data acquisition in 2011, the extension

Table 3.2.: Overview of meteorological derivatives until DOY 175.

	Abbr.	unit	2010	2011	2012	2013	2015
Start of Phenological Season	SOPS	DOY	114	97	119	107	122
Growing Days	GD	#	61	78	56	68	53
Growing Degree Days (T>5°C)	GDD5	#	33	48	36	34	43
Summarized Temperature	T	°C	366.9	454.3	399.7	377.2	395.9
Global Radiation	GR	W/m^2	12930	18877	14469	14941	12647
Days with Precipitation	PD	#	35	37	32	40	31
Total amount of Precipitation	PT	mm	170.3	242.3	184	251.2	208.9
Sunshine Duration	SD	h	277.8	485	343.7	290.7	281.4

of the mosaic is smaller in this year than in the others. Therefore, all mosaics of the other years were resized to the extent of 2011 (E:2800683/N: 1165001 to E: 2803761/N: 1161549). Subset and mosaic generation was performed using the commercially available software ENVI 5.2 (Exelis Visual Information Solutions, Boulder, Colorado).

3.2.1.3. Data Co-Registration

By comparing the mosaic of the individual years, discontinuous displacements of the images of up to tree pixels ($6m$) are recognizable. These shifts are usually corrected by setting tie points in the images to be co-registered. Unfortunately, in high alpine regions there are often too few clearly distinguishable objects which allow the setting of proper tie points. In the present scenes only shade offers identifiable points for co-registration. Since the acquisition times between the years vary up to $270min$, the shade moves and these features are not usable as tie points (Figure 3.4). Therefore, the shifts could not be corrected and the test sites must consequently be selected manually for comparison between the years.

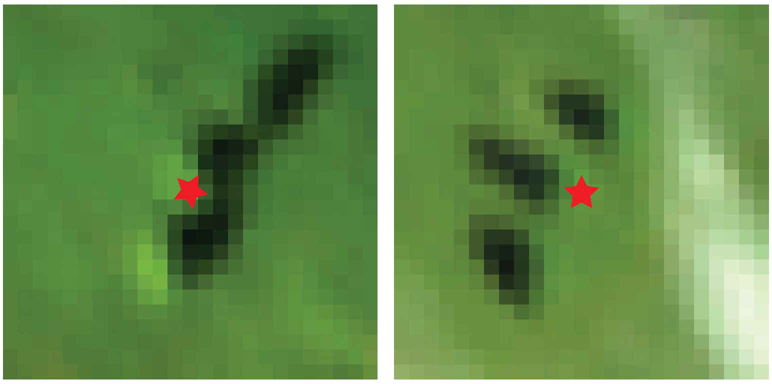

Figure 3.4.: Close-up of a tree group. The red asterisk indicates the same tree in the acquisition of 2011 around 3 p.m. (left) and in 2012 around 10.45 a.m. (right). The shade moves roughly 90°.

3.2.1.4. Land Cover Mapping

To separate land cover classes different approaches can be used. In this Master's Thesis a linear spectral unmixing (LSU) approach was used to find pure endmembers. LSU is a well approved approach to determine classes (Nichol and Wong, 2007; Smith et al., 2007). Endmembers were selected to distinguish between soil, grassland, rock, forest, snow and cloud. By applying a LSU approach, every pixel is decomposed in a collection of constituent spectra which indicates the fraction of each endmember presented in the pixel (Keshava and Mustard, 2002). LSU was mainly applied to the dataset of 2011. For cloud detection, data from 2012 and 2015 were used.

Cloud Mask Generation For a proper analysis of vegetated parts, cloudy parts must be excluded. For the sake of a complete land cover map, clouds and snow have to be differentiated. The selected endmembers of clouds and snow were not pure enough to differentiate between these two classes with a LSU. The use of Normalized Differenced Snow Index (NDSI) alleviates this issue and facilitates the discrimination between snow and clouds. The index is defined as follows:

NDSI=$\frac{TM_{band2}-TM_{band5}}{TM_{band2}+TM_{band5}}$

As evident within the formula, the NDSI was originally developed for the Landsat Thematic Mapper (TM) sensor, motivated by the large discrepancy between snow (nearly zero) and clouds (high values) in TM band 5 (Hall et al., 1995). Since the present thesis deals with APEX imagery instead, the bands in the NDSI had to be approximated by the closest hyperspectral bands. Suitable substitutes for TM bands 2 and 5 were identified at wavelengths of $0.5177\mu m$ and $1.6153\mu m$, respectively.

Unfortunately, the discrimination between clouds and background was still difficult because part of the rivers were reflecting similar to clouds. With additional visual assessment and manual selection, a sufficient cloud mask was created. The cloud mask was calculated for the data sets of 2012. The clouds in 2015 were dissolved after mosaicking.

Forest Mask Generation It emerged to be difficult to find endmembers of trees. There are no closed-canopy forests in the SNP; trees often stand in lines up at hillsides instead. Hence, single trees are mainly recognizable through their shade in the used APEX IS data set. Endmember selection for trees, tree shade and grassland did not discriminate trees from their shade properly. Therefore the forest mask was created through selecting visually discernible forested areas instead. Since forest stands in upper Val Trupchun are not dense, manual sampling of forest test sites in this area might not result in tree spectra (see Test Site Selecting). In the end, the forests mask contained also tree shade and grassland.

Grassland Mask Generation The selection of pixels with a grassland fraction greater than 0.35 led to an overall acceptable result, except for misclassifications at open soils at higher altitudes and depressions on hillsides. These pixels could be removed by including pixels with a soil fraction of less than 0.59. As mentioned before, single trees were also classified as grassland. Therefore, parts of grassland inside the forest mask were excluded from the grassland mask.

3.2.1.5. Test Site Selection

Due to the spatial shift between the years (see Section II. A. 3.), small test sites within the forest and grassland mask were selected manually. In general, statistically representative sample sizes consist of 30- 40 measurements. This sample size is found to be appropriate to detect infield radiometrically variation of vegetation (Kneubühler, 2002). For this study, 35 test sites per class were selected. Each test site includes $3x3$ pixels ($6x6m$).

Forest Test Site Selection Forest test sites were chosen by height, dispersion and tree composition and lay within the disjoint set of the forest and cloud masks (i.e., only patches covered by the forest mask, but not by the cloud mask were selected). From the complete set of over 60 test sites in the forested area, 35 test sites were selected according to the following rules: first, the altitude of pixels within the$3x3$ patches needed to feature a standard deviation score of at most $1.5m$. Second, the tree species was required to reflect the most typical species distributions within the area. Candidate patches were therefore compared to the SNP geographic informations system (GIS) inventory, which includes information about tree compositions (Schmid, 2016). Test sites with ratios between 100% larch inventories up to 50/50% larch/stone pine inventory were selected.

Grassland Test Site Selecting As for the forest test sites, grassland test sites were selected by altitude and dispersion over the hillslopes. First, over 90 test sites were selected. The primal criterion for inclusion was the altitude standard deviation, being no larger than $1.7m$. A second criterion was a sufficiently well-balanced selection between north-east and south-west aspect. Under these restrictions 35 test sites remained.

3.2.1.6. Vegetation Classes Generation

Different vegetation classes were built (see Table 3.3) with a sample size of at least 5 samples per class. For the forest, a class with all values (AF) was built with 35 samples. The class forest north-east (FNE) includes 26 samples, forest south-west (FSW) 9 samples. The five test sites with the highest larch percentage (100% to 80% larch) were grouped together to larch 92 (L92). The same was done for larch 70 (L70) (70%, 13 samples), larch 60 (L60) (60%, 12 samples) and larch 50 (L50) (50%, 5 samples). In All Grassland (AG), 35 test sites are represented. 15 grassland test sites have a north-eastern aspect (GNE) and 20 a south-western (GSW).

For some further calculations, the vegetation classes in their entirety were used (e.g. All test sites forest, AF, sample size 35). For comparability with meteorological derivatives, an average value per year for the respective vegetation class was calculated (e.g. averaged All Forest, aAF, sample size 5).

3.2.2. Calculation of Vegetation Indices

All applied VIs were developed for multispectral broadband sensors (e.g. Landsat TM). Using the hyperspectral band closest to the center wavelength of the broadband sensor has proven to be a solid method (Table 3.4) (Psomas et al., 2011; Verrelst et al., 2008). For all five years and all forest and grassland test sites NDVI, SR, NDWI, SAVI, MSAVI2, and NCI were calculated.

3.2.3. Statistical Analyzes

The use of statistical methods allows to test whether correlations of VI values of vegetation classes and meteorological data are significant. In addition, statistic enables to test if differences between means of vegetation classes are significant. All statistical analyses were carried out using SPSS (IBM SPSS Statistics Version 21).

3.2.3.1. Test for Normal Distribution

The data were tested for normal distribution using the Kolmogorov–Smirnov test. Depending on the test size a different significance level is defined (e.g. sample size of 35 =0.2224, see Appendix A.1). The tested values are normally distributed if the associated significance values are higher than the pre-set significance level (Brosius, 2011).

Table 3.3.: Selected vegetation classes with description, abbreviation, sample size and height information.

Vegetation Class	All values			Average		
	Description	Abrr.	sample size	Description	Abrr.	Sample size
All Forest	All test sites forest	AF	35	Averaged all test sites forest	aAF	5
Forest NE	Forest with north-east aspect	FNE	26	Averaged forest with north-east aspect	aFNE	5
Forest SW	Forest with south-west aspect	FSW	9	Averaged forest with south-west aspect	aFSW	5
Larch 92	Forest with 92% larch percentage	L92	5	Averaged forest with 92% larch percentage	aL92	5
Larch 70	Forest with 70% larch percentage	L70	13	Averaged forest with 70% larch percentage	aL70	5
Larch 60	Forest with 60% larch percentage	L60	12	Averaged forest with 60% larch percentage	aL60	5
Larch 50	Forest with 50% larch percentage	L50	5	Averaged forest with 60% larch percentage	aL50	5
All Grassland	All test sites grassland	AG	35	Averaged all test sites grassland	aAG	5
Grassland NE	Grassland with north-east aspect	GNE	15	Averaged grassland with north-east aspect	aGNE	5
Grassland SW	Grassland with south-west aspect	GSW	20	Averaged grassland with south-west aspect	aGSW	5

Table 3.4.: Overview of the used VIs with their abrrevation, calculation, used wavelengths and references.

Vegetation index	Abrr.	Formula	Used wavelenghts [µm]	Reference for vegetation index
Normalized Difference Vegetation Index	NDVI	$=\frac{NIR-RED}{NIR+RED}$	NIR = 0.864 RED = 0.671	(Rouse et al., 1974)
Simple Ratio	SR	$=\frac{NIR}{NIR}$	NIR = 0.864 RED = 0.671	(Jordan, 1969)
Normalized Difference Water Index	NDWI	$=\frac{nNIR-fNIR}{nNIR+fNIR}$	nNIR = 0.864 fNIR = 1.245	(Gao, 1996)
Soil Adjusted Vegetation Index	SAVI	$=\frac{NIR-RED}{NIR+RED+L}+1+L$	NIR = 0.864 RED = 0.671 L = 0.5	(Huete, 1988)
Modified Soil Adjusted Vegetation Index	MSAVI2	$=\frac{2*NIR+1-\sqrt{(2*NIR+1)^2-8*(NIR-RED)}}{2}$	NIR = 0.864 RED = 0.671	(Qi et al., 1994)
Normalized Canopy Index	NCI	$=\frac{MIR-GREEN}{MIR+GREEN}$	MIR = 1.665 GREEN = 0.545	(Vescovo and Gianelle, 2008)

All vegetation class VI values were tested for normal distribution as well as the averaged vegetation class VI values and the meteorological derivatives.

3.2.3.2. Correlation of Classes

To test the power of connection between two variables a correlation analysis was performed (Brosius, 2011). It is a premise to do a correlation test analysis that the data are on an interval or ratio scale. Furthermore, the knowledge about the distribution of the data decides on whether to use a parametric or non-parametric correlation analysis. For normally distributed data, a Pearson's correlation can be carried out; data following another, possibly unknown distribution require a transformation into ranks and hence Spearman's rho correlation instead (Brosius, 2011). Correlation coefficients range in both cases from 0 (no correlation) to 1 (perfect positive correlation) or -1 (perfect negative correlation) with steps in between (Brosius, 2011) (see Appendix A.2).

To test if VI values correlates with temperature the auxiliary quantity of height was used. Because there are no temperature data of different altitude levels, the well-known linear decrease of temperature with height of $0.5°C$ for $100m$ was assumed.

Correlations of altitude and AF VI values and AG VI values as well as meteorological derivatives and aAF VI values and aAG VI values were calculated.

3.2.3.3. Differences Between Classes

To test on differences between means of classes, an independently sampled t-test was done (Brosius, 2011). An important prerequisite to the t-test is the homogeneity of variances between the two investigated classes. This can be tested by Levene's test of similarity of variances (null hypothesis: variances are the same in both test sets).

The t-test has been carried out between FNE and FSW, GNE and GSW as well as between L92, L70, L60 and L50, respectively. After finding differences between means of the vegetation classes, a second round of t-tests was carried out between the averaged means of classes aFNE and aFSW, aGNE and aGSW and between aL92, aL70, aL60 and aL50.

In addition, in case of finding differences between means of classes (e.g. between aFNE and aFSW), a correlation test analysis of meteorological derivatives and aFNE and aFSW was applied to the mentioned samples. The same sequence was performed for aGNE and aGSW as well as for aL92, aL70, aL60 and aL50.

4. Results

In this section, the most important results are presented. Meteorological derivative distributions are shown introduced. Preprocessed data like mosaics, data co-registration, land cover mapping and test site selection are depicted. The calculated vegetation indices are reviewed. Correlations of vegetation classes, meteorological derivatives and limiting constraints as well as differences between vegetation classes are presented.

4.1. Data

The APEX IS and meteorological data are already comprehensively discussed in the methods section. This section describes the response to meteorological derivatives explaining the distribution among the years.

Meteorological conditions differ for every year analyzed in their characteristics and extremes. In the period between 2010 and 2015, the highest values can be observed in 2011 for most of the meteorological derivatives (Figure 4.1). GD, PD and PT show an "M"-shaped figure among the years with higher values in 2011 and 2013 and lower values in 2010, 2012, and 2015 (denoted as "M"-shape further below). GR, SD, T and, to some extent also GDD5 peak in 2011, followed by lower values.

4.2. Data Preprocessing

In this section, the results of selected processing steps are presented and the chosen test sites are illustrated.

4.2.1. Building Subsets and Mosaics

The mosaics from 2010 to 2015 are presented in Figure 4.2. Comparing the mosaics, a clear difference between 2011 and 2013 depending on the available sectors can be seen.

4.2.2. Land Cover Mapping

The final masks for clouds, forest and grassland are presented in Figure 4.3. The full area of upper Val Trupchun covers $5.32km^2$, of which $0.175km^2$ are forest, $1.287km^2$ grassland and $0.189km^2$ area covered by clouds.

4.2.3. Test Site Selection

The selected test sites in the forest and in grassland are presented in Figure 4.4.

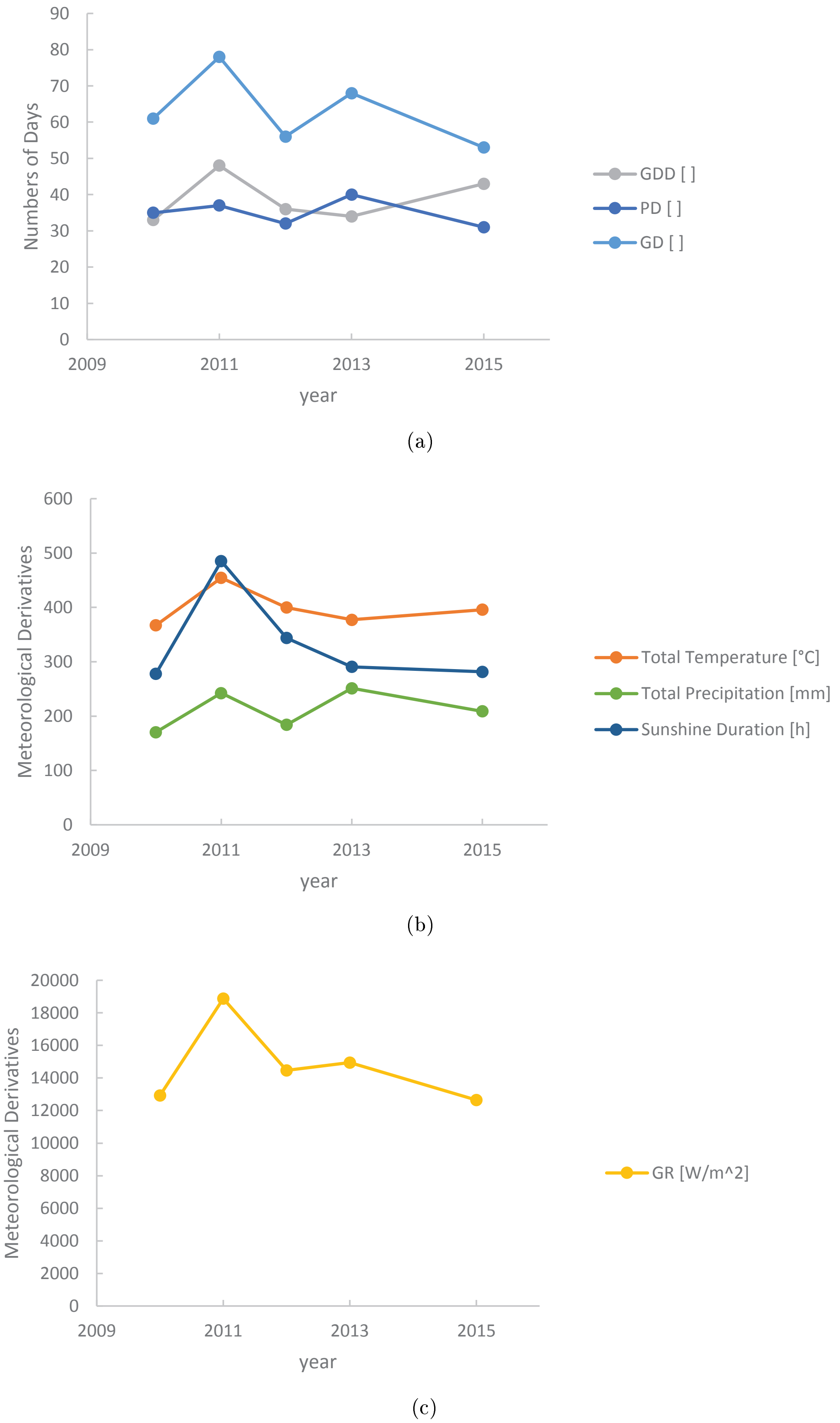

Figure 4.1.: Meteorological derivatives summarized from SOPS to DOY 175 (a) and individual units (see brackets) summarized from SOPS to DOY 175 (b) and (c).

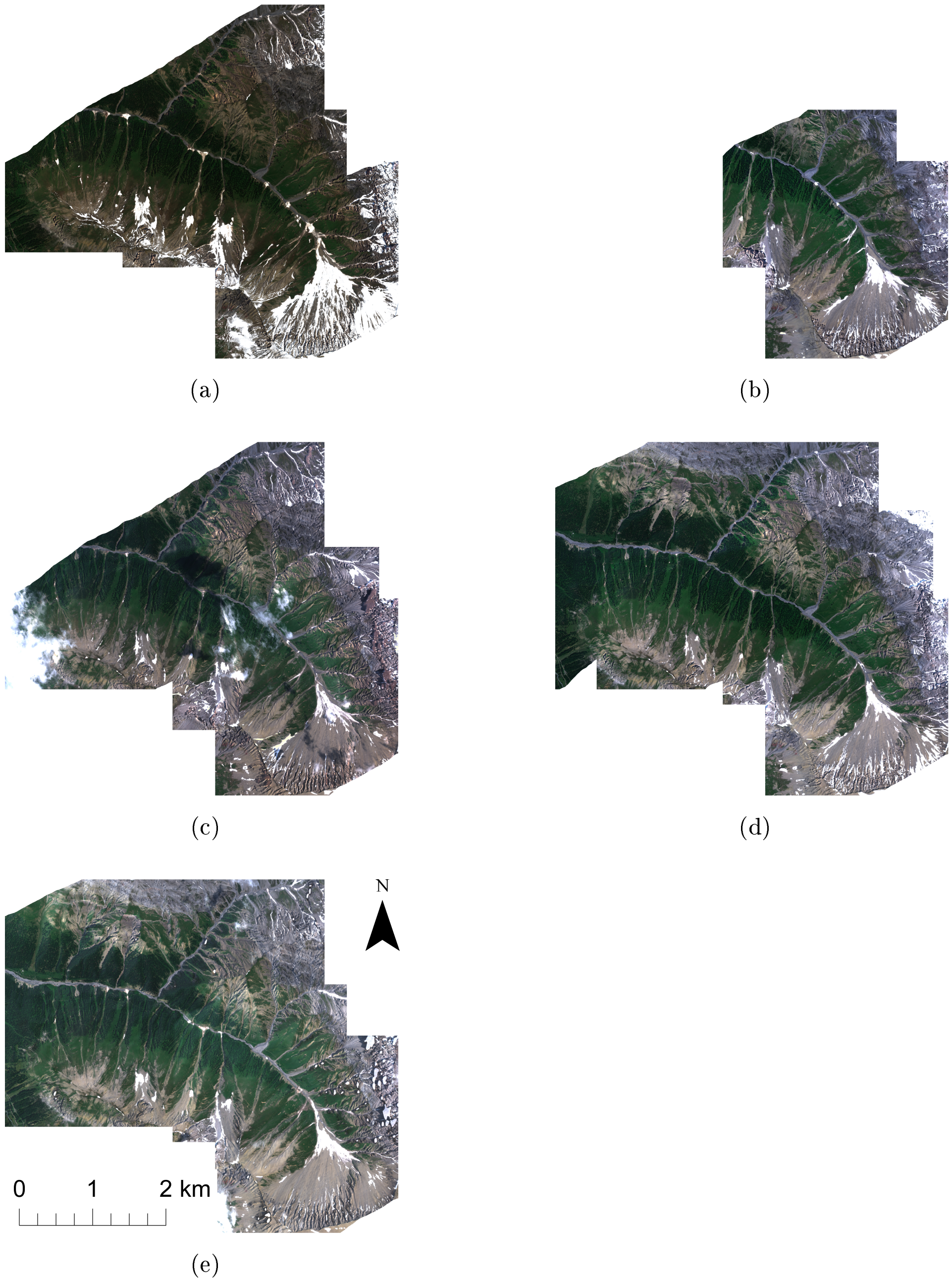

Figure 4.2.: Mosaics of different sectors, (a) 2010, (b) 2011, (c) 2012, (d) 2013 and (e) 2015 (scale of e also applies to a-d).

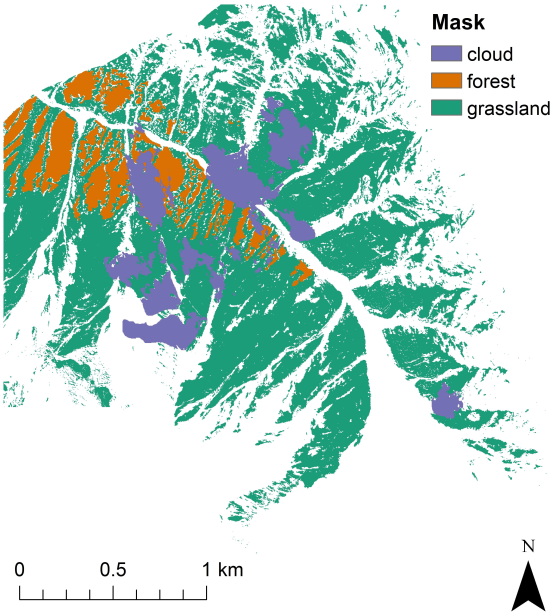

Figure 4.3.: Applied land cover mask in the upper Val Trupchun.

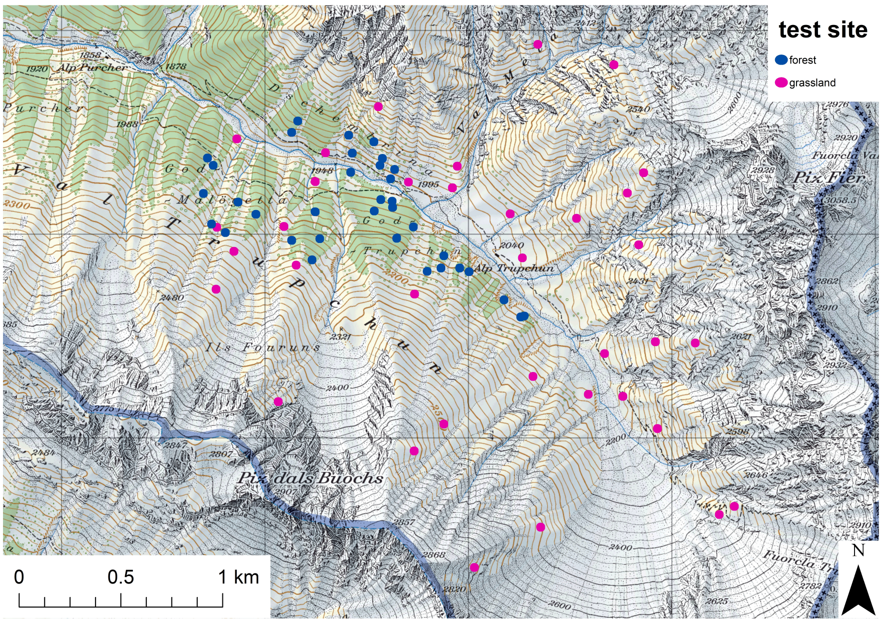

Figure 4.4.: Selected test sites for forest and grassland in Val Trupchun. (source background map: Bundesamt für Landestopographie, Switzerland).

4.3. Vegetation Indices Calculation

All VIs were calculated for each year from 2010 to 2015. Being representative for all VIs, the results for the NDVI can be seen in Figure 4.5.

Figure 4.6 displays boxplots of VIs for all forest test sites and years. VIs vary in the forest test sites, showing higher mean values in 2011 and 2013 and lower mean values in 2010, 2012 and 2015 implicating an an "M"- shape (MSAVI2, NDVI, SAVI and SR). For MSAVI2, there are three mild outliers (test site 3 (2012), 9 (2010) and 15 (2012)). The same mild outliers were also found in NDVI and SAVI. Furthermore, the distribution of test site values was similar among the years, only the range of values differs from VI to VI. NDWI shows different results: Test site 20, 22 and 31 as extreme outliers (asterisks) show considerably lower values than the rest of the data. In addition, the "M"-shape was not visible. The data range and distribution were relatively stable. The NCI shows decreasing means from 2010 to 2015.

For all grassland test sites, boxplots for all years and VI values were calculated (Figure 4.7). VIs vary in the grassland test site showing higher mean values in 2011 and 2013 and lower mean values in 2010, 2012 and 2015, implicating an "M"- shape similar to the forest sites (MSAVI2, NDVI, SAVI and SR). MSAVI2, NDVI and SAVI show mostly the same outliers (test sites 23 and 27), but the boxplots are more extended. The MSAVI2 2013 est site 15 was also an outlier. The NDWI shows one extreme outlier at test site number 35, the median slightly increases from 2010 to 2015. The NCI decreases from 2010 to 2015.

4.4. Statistical Analysis

4.4.1. Analyzing the Distribution

All datasets listed in Table 4.1 were tested on normal distribution for each year and VI, with the averaged values from 2010 to 2015. Nearly all tested VI data as well as the meteorological data are normally distributed with the exception of NDWI values and one time NCI value.

4.4.2. Analyzing the Correlation of Classes

Detailed results for correlations of temperature and aAF and aAG as well as between GD, GDD5, T, GR, PD, PT, SD and aAF and aAG can be found in the following sections. The differences between FNE and FSW as well as GNE and GSW, their averages aFNE, aFSW, aGNE, aGSW as well as between the different larch classes L92, L70, L60, L50 are also presented.

4.4.2.1. VI Diminishing with Temperature

The VI values (2010 to 2015, averaged for every test site) are presented in relation to their altitude (Figure 4.8). The depicted trend lines show a slight decrease of the values with increasing altitude for forest test sites and a slightly stronger decrease for grassland test sites for MSAVI2, NDVI, NDWI, SAVI and SR. Only the NCI trend line shows a weak increase with altitude for forest as well as for grassland test sites.

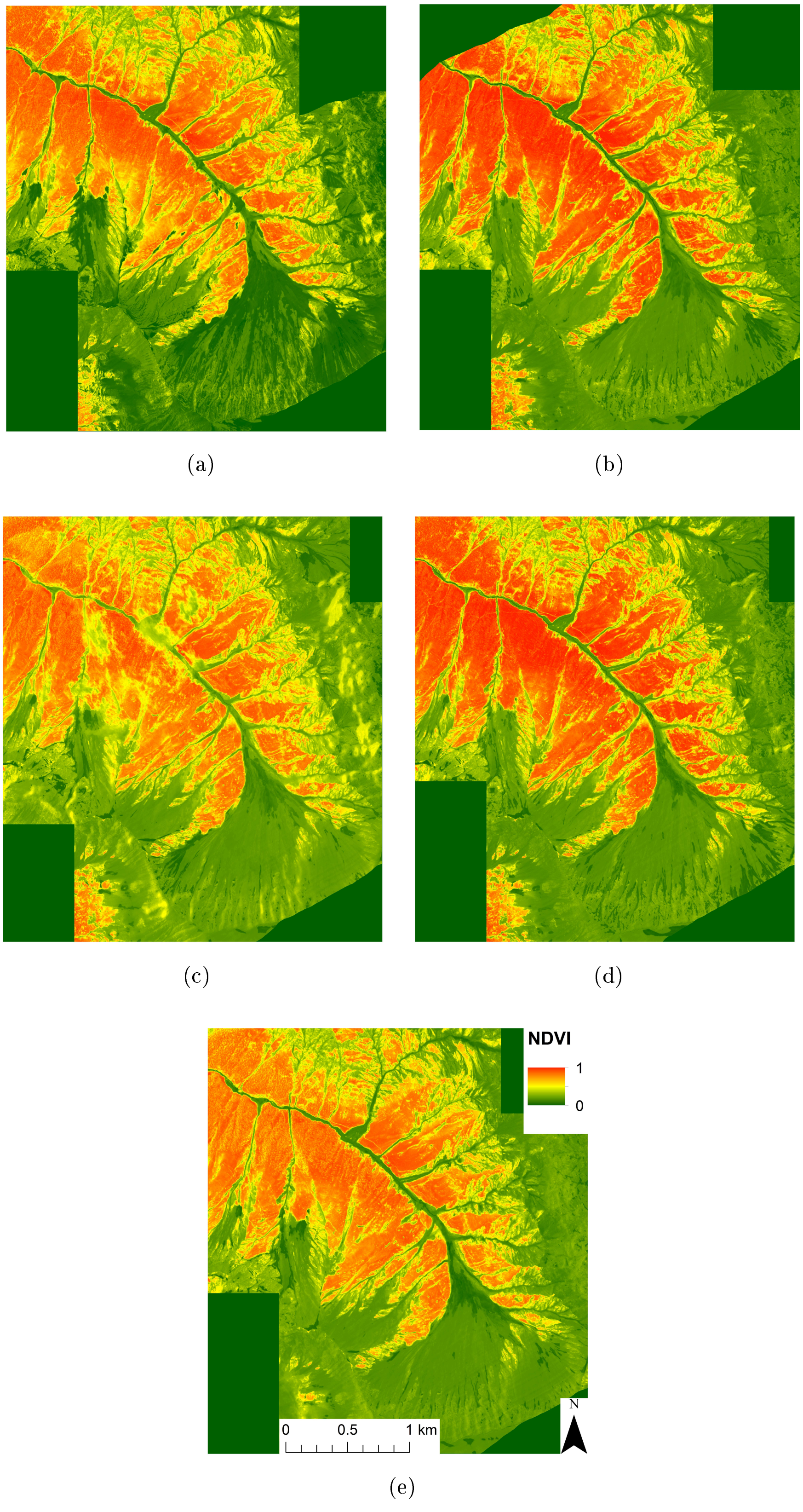

Figure 4.5.: Maps of NDVI values in (a) 2010, (b) 2011, (c) 2012, (d) 2013, (e) 2015. All maps use the same color code (values smaller than 0 are adapted to 0; spatial scale of e also applies to a-d).

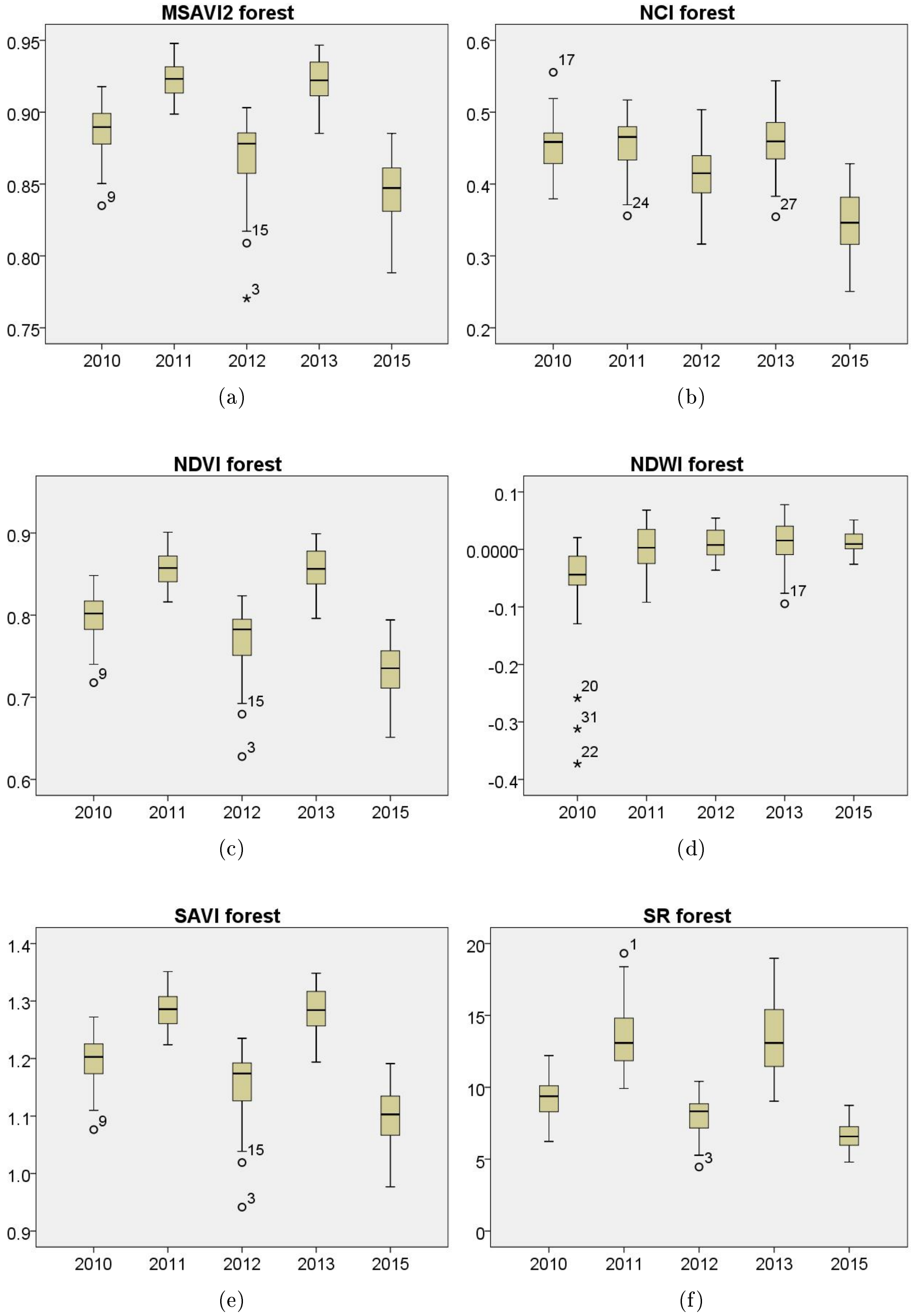

Figure 4.6.: VI values in the forest sites from 2010 to 2015, the y axis showing the respective VI. Boxes indicate interquartile range crossed by horizontal bars representing the median. The whiskers span was 1.5x the interquartile range. Mild outliers represented by curls lay in the 1.5x to 3x interquartile range. Asterisks representing extreme outliers are far off 3x interquartile range. Point numbers correspond to sample numbers.

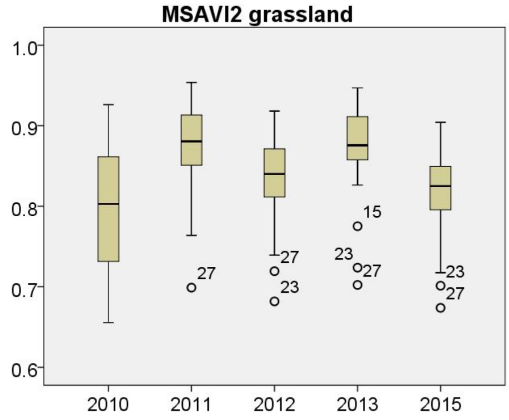

(a)

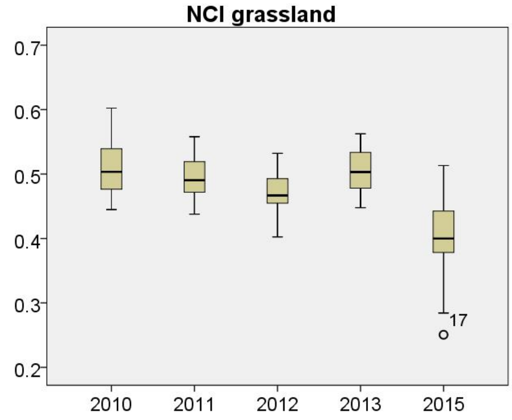

(b)

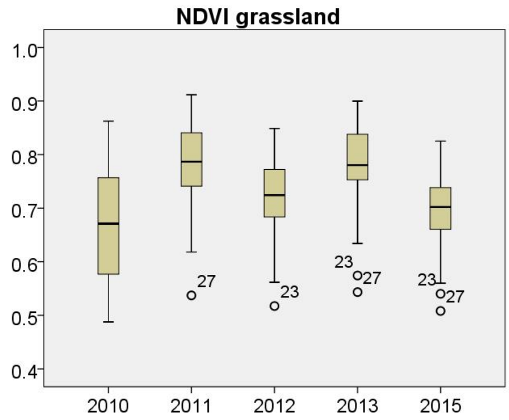

(c)

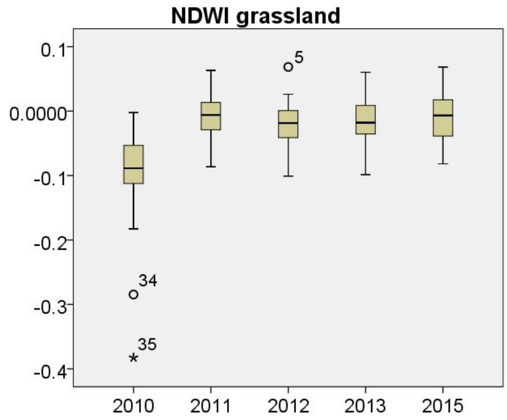

(d)

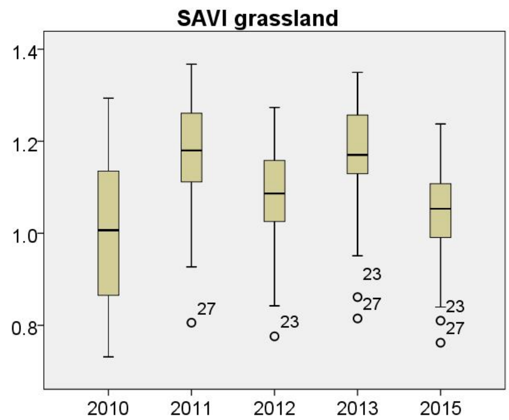

(e)

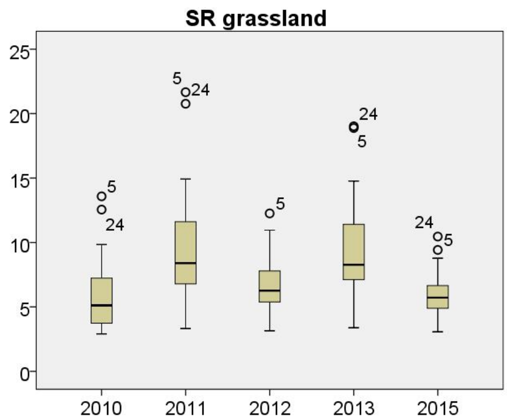

(f)

Figure 4.7.: VI values in the grassland sites from 2010 to 2015, the y axis showing the respective VI. Boxes indicate interquartile ranges crossed by horizontal bars representing the median. The whiskers span was $1.5x$ the interquartile range. Mild outliers represented by curls lay in the $1.5x$ to $3x$ interquartile range. Asterisks represent extreme outliers that are far off the $3x$ interquartile range. Point numbers correspond to sample numbers.

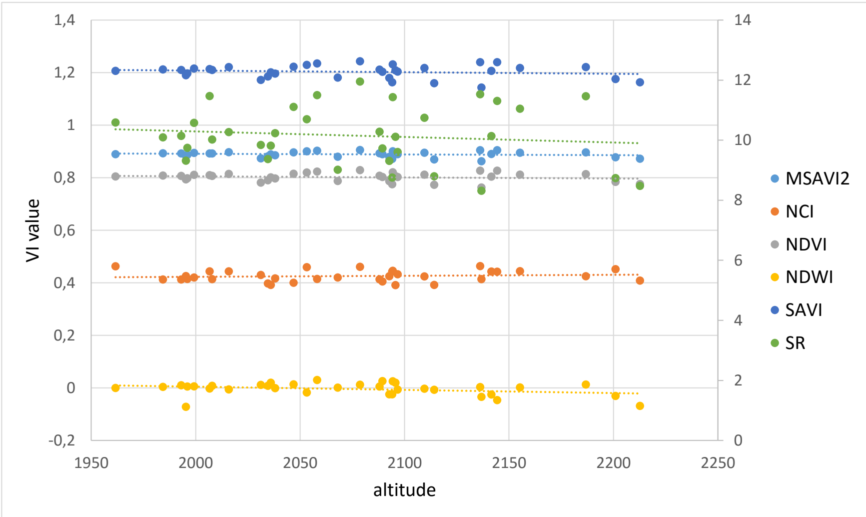

(a)

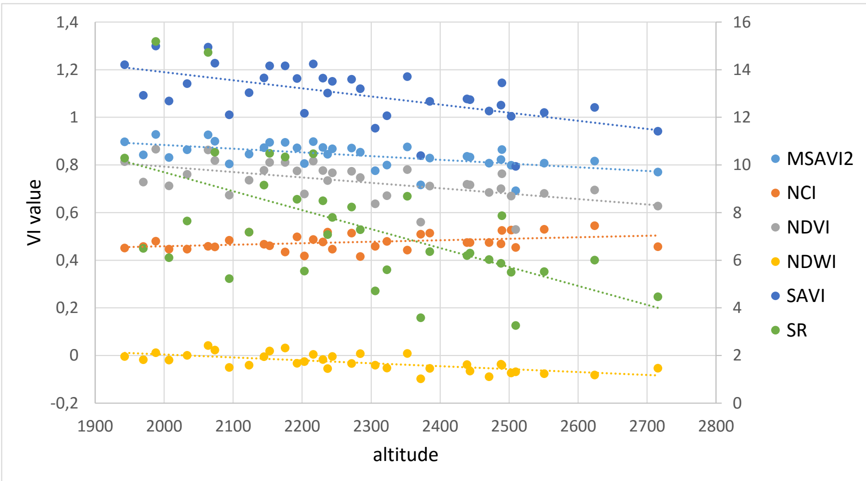

(b)

Figure 4.8.: (a) VI values 2010 to 2015, averaged for every test site for forest. (b) VI values 2010 to 2015, averaged for every test site for grassland.

Table 4.1.: Results of the Kolmogorov-Smirnov test for normal distribution. Displayed are the not normal distributed VI values which have been calculated.

	sample size (n)	Kolmogorov-Smirnov critical value	asymptotic significance (two tailed)
2010 NDWI forest	35	0.2242	0.004
NDWI forest mean	5	0.5633	0.309
NDWI grassland mean	5	0.5633	0.379
NDWI larch 60	5	0.5633	0.497
NDWI forest north-east	5	0.5633	0.414
NCI forest south-west	5	0.5633	0.393
NDWI grassland north-east	5	0.5633	0.4
NDWI grassland south-west	5	0.5633	0.419

The correlation of VI values in the forest with their auxiliary quantity of altitude was presented in Table 4.2. There was only a significant correlation of altitude and auxiliary VI value for two years. Additionally, the correlation was weak (MSAVI2 forest, -0.301). There was however a positive weak correlation of NCI of 0.373 with increasing altitude.

All VIs, excluding NCI, of grassland test sites correlate significantly with altitude Table 4.3. The averaged VIs shows a moderate correlation (values between -0.53 and -0.569). As already described for forest, there was a negative correlation for all VIs with increasing altitude. The only exception was NCI which positively correlates with increasing altitude (value of 0.498).

Table 4.2.: Correlation of VI values and associated altitude values for forested test sites. The numbers of significant values indicate the numbers of years with significant values.

	numbers of significant values	averaged significant correlation coefficients (R)
MSAVI2 forest	2	-0.301
NCI forest	1	0.373
NDVI forest	2	-0.306
NDWI forest	2	-0.499
SAVI forest	2	-0.306
SR forest	2	-0.349

Table 4.3.: Correlation of VI values and associated altitude values for grassland test sites. The numbers of significant values indicate the number of years with significant values.

	numbers of significant values	averaged significant correlation coefficients (R)
MSAVI2 grassland	5	-0.530
NCI grassland	2	0.498
NDVI grassland	5	-0.542
NDWI grassland	5	-0.569
SAVI grassland	5	-0.542
SR grassland	5	-0.563

Table 4.4.: Correlations of VI values and selected meteorological derivatives, averaged over all years. Only significant correlation coefficients (R) are shown.

mean over years	GD	PD	PT
MSAVI2 forest	0.929	0.938	
NDVI forest	0.931	0.940	
SAVI forest	0.931	0.940	
SR forest	0.942	0.937	
MSAVI2 grassland			0.894
NDVI grassland			0.897
SAVI grassland			0.897
SR grassland	0.879		0.895

4.4.2.2. Correlating Averaged VI Values with Meteorological Derivatives

The significant results for the correlation of meteorological derivatives (GD, GDD5, T, GR, PD, PT, SD) with averaged vegetation classes (aAF, aAG) VI values are listed in Table 4.4. Very strong and positive correlations for aAF with GD are reported for MSAVI2, NDVI, SAVI and SR (R values higher than 0.929). For aAG, only SR shows a very strong positive correlation of 0.879 with GD. Precipitation was significant for both vegetation classes. MSAVI2, NDVI, SAVI and SR for forest correlate strongly to PD with positive correlation values over 0.937. In contrast, PT correlate strongly in the grassland case with the same VIs with values higher than 0.894.

4.4.3. Differences Between Classes

Differences between two or more subclasses of a vegetation class allow for further statistical analysis. The results of difference of means calculations of VI values with FNE and FSW as well as GNE and GSW are presented below. The VI values of the different forest tree compositions (L92 L70, L60, L50) have also been tested on differences between the individual classes.

Table 4.5.: VI values of the forest and grassland separated in two aspect groups (north-east and south-west). Levenes test: values above 0.05 represent variance homogeneity. T-test differences of means between aspects: values above 0.05 indicate no difference between the aspect classes.

	levenes	t-test differences of means between aspect
NCI 2010 forest	0.798	0.017
MSAVI2 2012 forest	0.031	0.002
NDVI 2012 forest	0.029	0.002
SAVI 2012 forest	0.029	0.002
SR 2012 forest	0.056	0.016
NCI 2013 forest	0.810	0.016
NCI 2015 forest	0.448	0.000
SR 2015 forest	0.007	0.004
NCI 2010 grassland	0.394	0.000
MSAVI2 2011 grassland	0.119	0.018
NCI 2011 grassland	0.318	0.015
NDVI 2011 grassland	0.145	0.017
SAVI 2011 grassland	0.145	0.017
NCI 2012 grassland	0.005	0.019
NCI 2013 grassland	0.255	0.001
NCI 2015 grassland	0.565	0.000

4.4.3.1. Analysis of VI Values with Different Aspect

The test of differences of means between the two sampled groups (NE and SW aspect) was made for every year and every VI. Significant t-test results are listed in Table 4.5. The VI resulting in most frequent differences over the years between the two groups appears to be NCI, being significant in 2010, 2013 and 2015 for forest and all years for grassland. All other presented VIs shows significant difference only for two years at maximum.

To finally correlate differences in the aspect with meteorological derivatives the vegetation classes FNE, FSW, GNE and GSW VI values had to be averaged on a yearly basis to be comparable with the five years of meteorological data. For forest as well as for grassland homogeneity was found in the variances and no significance for differences between aspect north-east and south-west. The absence of difference between the averaged aspect classes makes a correlation analysis needless.

4.4.3.2. Analysis of Averaged VI Values with Different Tree Compositions

The forest classes with different larch percentage (L92, L70, L60, L50) showed variance homogeneity, no difference of means between the tested classes was significant. Therefore, further analysis of differences of means between averaged tree percentage classes and correlations with meteorological data allow no further findings.

5. Discussion

5.1. Data

To estimate above ground green biomass or phenological development with VIs from RS data, the acquisition date is essential. In the beginning of the phenological season, VIs are influenced by a mixture of background and standing litter (Halabuk et al., 2013). In the early summer (end of June to July) litter is still there but vegetation has already overgrown, so that VIs response represents phenological development. Data acquisition for this study took place between end of June and begin of July and is therefore adequate for phenological research.

5.1.1. Meteorological Derivatives

Nearly all meteorological derivatives (GD, GDD5, T, GR and SD) show a maximal peak in the year 2011. This can be explained with SOPS in 2011 at DOY 97 the longest extended GD period. The second peak is present in 2013 in which GD and especially PT and PD show higher values. The temporal trend of GDD5 expectably coincides with the course of T, as the two are directly related. The higher values of GD and GDD5, T, GR and SD suggest that climatic conditions allowed advanced phenological development in spring 2011 compared to the other years, which coincides with the findings of Kneubühler et al. (2014).

5.2. Methods

5.2.1. Test Site Selection

Test sites were selected in a consistent manner with a restricted altitude standard deviation in the test site of less than $1.7m$ for grassland and less than $1.5m$ for forest and dispersed over the area and with different aspect. The sample size is appropriate (Kneubühler, 2002) and the $3x3$ pixels forming the test sites sufficiently diminish effects of shifts between the APEX IS data. The selected test sites are surveyed on consistency and usefulness on 2011 APEX IS data and proved to be sufficient.

5.2.2. Vegetation Indices Calculation and Application

As mentioned in the results (II.C.1.), most of the VIs show only mild outliers, with NDWI being the only exception. In 2010, NDWI data has a value span of 0.395 for forest and 0.380 for grassland. In all other years the differences between the highest and lowest values are smaller than 0.17. The reason for these extreme outliers is based on the selection of test sites. For both forest and for grassland the outlier test sites (forest: 20, 22, 32; grassland 34, 35) are located where the calibration wire of APEX

IS causes the data voids (Jehle et al., 2010). The calibration wire is interpolated in the data and not visual in most of the spectral bands. Unfortunately, the calibration wire is poorly interpolated in the 2010s near infrared bands (also at $1.245\mu m$) and therefore clearly visible. Therefore, the values at position under the calibration wire do not represent correct values for the NDWI calculation in 2010. The poor performance of NDWI reduces the comparability with the other VIs used in this thesis. In fact, NDWI is chosen as robust VI in alpine vegetation because standing litter does not influence the resulting value due to sensitivity to plant water (Halabuk et al., 2013). For the mentioned reasons this cannot be confirmed in this study.

The boxplots of nearly every VI present an “M”-shape. The same “M”-shape exists in the meteorological derivatives. In fact, the high values in the 2013 VIs stand out because in the meteorological derivatives GDD5 and T are extremely low. This discrepancy could probably be explained with the acquisition time of APEX IS data at July 12. Between the meteorological end date DOY 175 and the APEX IS data acquisition date, 18 days passed in which phenology had time to develop.

For NCI and NDWI, the distribution is only slightly “M”-shaped. For NCI a decreasing tendency can be seen over the years, whereas the opposite trend is present within the data for NDWI. This pattern cannot be explained with meteorological derivatives.

5.2.3. Statistical Analysis

5.2.3.1. Analysis of Distribution

The averaged data are normally distributed with exception of forest and grassland NDWI. Averaged NDWI values are not normally distributed, potentially because of the already mentioned calibration wire (II.B.) of the APEX IS data. If the test sites forming outliers in 2010 for NDWI are excluded in the Kolmogorov-Smirnov calculation, the data are normally distributed.

The normal distribution of the VIs allows for their use in statistical analysis because this indicates no saturation. A sharp right hand shoulder in a histogram (not shown in this study) of a VI indicates saturation (Huete et al., 2002). Saturation effects occur when the amount of above-ground green biomass is too high.

5.2.3.2. Analyzing the Correlations of Classes

Diminishment with Temperature The 5-year averaged VI values for test sites slightly decrease for nearly all VIs with increasing altitude. Differences in the inclination of the trend line can be observed between forest and grassland: grassland shows a stronger decrease than forest. The same pattern can be observed for the correlation of VI value of a site and its altitude. For forest test sites, the values of up to two years show significant and weak negative correlations. For grassland, the values for all five years are significant (excluding NCI values) with moderate negative correlations. Other studies also describe a decrease in NDVI with higher elevation which is probably caused by reduced vegetation productivity and cover (Chapman, 2013; Kariyeva and van Leeuwen, 2011). In contrast to forest, the grassland cover decreases with increasing altitude. Vegetation is getting sparse and more background gets visible. This leads to the assumption that temperature is for forest not an equally strong limiting factor for forest as it is for grassland.

In contrast to other studies, the correlation analysis for NCI presents a positive trend with increasing altitude. The studies that used NCI presented results with potential for biomass estimation of NCI (Vescovo and Gianelle, 2008; Yang et al., 2012). It is questionable if NCI is exclusively controlled by biomass, instead it can be supposed that NCI is sensitive to background substance (soil and rock).

Correlating of Averaged VI Values with Meteorological Derivative The results of VIs correlated with meteorological derivatives show clear dependences between VIs on one side and GD and precipitation on the other side. All other meteorological derivatives were not significant (GDD5, T, GR, SD). Surprisingly, there is a difference between forest and grassland responses to precipitation. The values for forests are very strongly correlated with PD, those for grassland instead with PT (MSAVI2, NDVI, SAVI and SR). This can be explained by the adaptive strategy of water use efficiency (Wang et al., 2003). The correlation with the amount of precipitation is also indicated in other studies for upper Yellow River Catchment in China (forest and grassland) and for Kansas (grassland) (Hao et al., 2012; Wang et al., 2003). In this study area, a proposed main constraint by water availability in high alpine regions can be confirmed as presented by (Wang et al., 2013).

As described in the introduction, GDD is an important parameter to monitor vegetation phenology and available heat for plants. In the study site upper Val Trupchun, GDD5 is not significantly correlated with VIs (at least during the years 2010 to 2015). The same result is found for T. This result does not coincide with findings for Nebraska in which the correlation of NDVI and GDD was strongly significant (Yang et al., 1997). The deviant results may be due to the fact that for Nebraska, GDD was calculated using minimum and maximum temperature with a minimal threshold of $10°C$. Because vegetation in alpine regions is adapted to a harsher climate, thresholds for GDD should be reviewed.

5.2.3.3. Analyzing Differences Between Classes

VI Values of Different Aspects Differences of means between the aspects are found for forest as well as for grassland. In particular, NCI is significant for forest for three years and for grassland for all five years. NCI may strongly be influenced by different illumination effects which could be an explanation for this very strong correlation over time and vegetation classes. The other interesting pattern is shown in 2012 for forest. MSAVI2, NDVI, SAVI and SR are significant in differences of means between the aspects NE and SW. A meaningful explanation for this is not found.

The averaged VIs show no differences between the aspect groups. Consequently, there is no dependence on factors of meteorological derivatives.

Averaged VI Values of Different Tree Compositions Between the different tree classes is no difference in composition found. It is well known that larch budburst occurs later as altitudes increases (Moser et al., 2010). But budburst had already happened at the acquisition dates. The adaption of tree species of a high alpine forest to climate may cause this result. There is no difference in means in early summer (end of June) between the tree classes in the forest.

5.3. Limitations of This Study

Unfortunately, an applied automatic co-registration for the five years mosaic was not feasible. Co-registered data sets would theoretically allow comparing single trees instead of entire forests. In this case, the selection of small-sized test sites would not have been necessary because the whole area of grassland or forest (single trees) could have been used for subsequent analyzes.

The different amount of APEX IS data over Val Trupchun led to the fact that in 2011 a limited area had to be chosen as study area. For vegetation comparability, it would have been interesting if the study are would comprise forest further down the valley because it is denser and would allow a wider range in altitude to be explored.

APEX IS data for 2010 were not available at the same preprocessing level as for the other years. This mainly impacts infrared bands in the range of 1.07 to 1.46μm. This lack is clearly observable for test site NDWI values and causes the non-normal distribution of NDWI. In 2010 data, a small line-artifact is visible between 1.29 and 1.46μm (2.8m cross section dimension) and a wide strip from 1.14 to 1.28μm (48.2m cross section dimension), where VI values behave unexpectedly. In recent state-of-the-art data the calibration wire is interpolated already in the preprocessed data.

Meteorological data were restricted by availability for Buffalora station. It would have been really interesting to have snowmelt and snow package data for every year. This would allow defining the start of season independently from temperature. The use of GDD5 in this study only allowed for an assumption of the start of the season. Furthermore, more meteorological stations located in the Val Trupchun would enabled a correlation analysis on test site level with the correspondent VI values.

Meteorological derivatives all have the same end date (DOY 175) because of comparability reasons. In 2013, the difference between DOY 175 and the acquisition date was 18 days. Due to the potentially strong phenological-driving impact of this period of time, the aggregated meteorological values do not really represent the initial phenology-meteorological position in 2013. For further calculation, it would be essential to review the use of 2013 data.

5.4. Research Questions

5.4.1. Are the VIs Linearly Correlated with Temperature?

Yes, the VIs for grassland and partly for forest are correlated with altitude and due to the linear dependence of temperature with altitude, also with temperature. The correlations of grassland VIs (MSAVI2, NDVI, NDWI, SAVI and SR) and altitude are moderate in every year. For forest, the correlations are weak in two of five years for the same VIs. A reason for this difference between the vegetation classes could be that grassland is getting sparse with higher altitude and soil and rock background visibility increases.

5.4.2. Are Differences Between VI Values of Vegetation Classes Linkable to Meteorological Derivatives and so to Environmental Constraints and Key Drivers?

Yes, there are differences in the VI values between the forest and grassland vegetation classes. The main difference applies to the very strong correlation of the numbers of days with precipitation and forest and also to the very strong correlation of the total amount of precipitation and grassland. Therefore, precipitation as part of the water availability constraint seems to be the main driver for alpine vegetation in the upper Val Trupchun. Additionally, forest correlates with GD. Correlations of vegetation classes and all other meteorological derivatives (GDD5, T, GR, SD) are not significant.

5.4.3. Are There Differences in VI Values Within Vegetation Classes Due to the Fact that There Are Different Terrain Aspects?

Yes, there are differences of means in vegetation classes VI values due to different aspects. The difference was clearly found between GNE and GSW test sites and partly in FNE and FSW. For averaged aspect data (aGNE, aGSW, aFNE, aFSW) no difference was found regardless of the sample aspect. This leads to the conclusion that meteorological derivatives are not correlated with the averaged VI values because there is no difference between the aspects.

5.4.4. Are There Differences in VI Values Between Forests with Different Tree Composition Depending on Environmental Constraints and Key Drivers?

No, there are no differences in the VI values between forests with differing tree composition.

5.4.5. Are the Chosen VIs Appropriate to Detect Differences Between Vegetation Classes in Alpine Regions?

Yes, the chosen VIs are appropriate to detect differences between classes in alpine regions. MSAVI2, NDVI, SAVI and SR specifically suited for change detection. NCI does not seem to be appropriate in alpine regions. The obtained values for NCI appear to be unreliable, e.g. NCI increases with height. NDWI cannot be definitely excluded due to limited test site selection.

5.4.6. Which of the VIs Performs Best?

In this study MSAVI2, NDVI, SAVI and SR performed on an adequate and comparable level, therefore they are appropriate for phenological observation in alpine regions. Furthermore, it is important to point out that no saturation effect could be found in the VI data. Hence, saturation does not constrain the selected VIs in high alpine regions. Most studies in literature use NDVI for correlation analyzes with meteorological data. For this reason the use of NDVI is recommended.

6. Conclusions

The correlation of meteorological data with different VI values of vegetation classes was tested in this Master's Thesis. APEX IS data sets of the different test sites of forest and grassland in the Swiss National Park (SNP) were explored. The analyses showed very strong correlations of VI values (MSAVI2, NDVI, SAVI, and SR) with precipitation. This result confirms the findings of other studies (Hao et al., 2012; Wang et al., 2003). In a similar study a strong relation between alpine regions and temperature is stated (Schultz and Halpert, 1993). The available data from SNP confirm a dependency from temperature but only in that way that VI values decreased with higher altitudes. No significant correlation of temperature and vegetation classes could be found.

APEX IS data from 2010 to 2015 allow a detailed study on the differences in VI values of vegetation classes. The quality of APEX IS data series is unfortunately damaged due to unsolved problems with co-registration and data preprocessing. The applied data nevertheless contain a wealth of spectral information and enable in-depth analysis of phenological development state.

Detailed correlation analysis of vegetation classes in high alpine regions with meteorological data bears the potential to improve the understanding of climate constraints in high alpine regions. Further climate constraint analysis may provide input parameters in high alpine regions for climate change modelling. Long-term multi-temporal data will help to correlate meteorological data with vegetation classes present in the SNP more robustly and probably confirm climatic trends.

7. Outlook

To further investigate the dependence of VI values for vegetation classes on meteorology data, some aspects need to be considered. An enhanced set of meteorological data is needed to correlate the specific test sites and meteorological data in more detail. Most important, there should be specific meteorological data for each test site. Precise information on the snowmelt data for each test site would further enable clarify SOPS. In this study the end date for meteorological data was chosen equal to the acquisition date in 2010 (earliest acquisition date). It could be a possibility to finally sum up the meteorological data to the real acquisition date every year. The comparability between the years will be more complicated, but meteorological values would better represent the effective meteorological condition in the particular year.

The NCI performed worse for alpine vegetation in this Master's Thesis than reported by other authors. Therefore, more research is necessary on NCI performance in rugged terrain with sparse vegetation cover.

If climate trend studies should be undertaken, the multi-temporal data acquisition needs to be expanded. It makes sense to continue the acquisition with APEX IS since reliable results were achieved. Long-term data sets are specifically needed to investigate the impact of climate change on vegetation.

Appendix

Bibliography

Austin, M. P., 1980. Searching for a model for use in vegetation analysis. Vegetatio 42 (1-3), 11–21.

Badeck, F. W., Bondeau, A., Böttcher, K., Doktor, D., Lucht, W., Schaber, J., Sitch, S., 2004. Responses of spring phenology to climate change. New Phytologist 162 (2), 295–309.

Bannari, A., Morin, D., Bonn, F., Huete, A. R., 1995. A review of vegetation indices. Remote Sensing Reviews 13 (1-2), 95–120.

Barati, S., Rayegani, B., Saati, M., Sharifi, A., Nasri, M., 2011. Comparison the accuracies of different spectral indices for estimation of vegetation cover fraction in sparse vegetated areas. The Egyptian Journal of Remote Sensing and Space Sciences 14 (1), 49–56.

Beniston, M., Rebetez, M., 1996. Regional behavior of minimum temperatures in Switzerland for the period 1979-1993. Theoretical and Applied Climatology 53 (4), 231–243.

Billings, W. D., Bliss, L. C., 1959. An alpine snowbank environment and its effects on vegetation, plant development, and productivity. Ecology 40 (3), 388–397.

Blumthaler, M., 2012. Solar Radiation of the High Alps. In: Lutz, C. (Ed.), Plants in Alpine Regions: Cell Physiology of Adaption and Survival Strategies. Vol. 1. Springer-Verlag Berlin, Berlin, Germany, pp. 11–20.

Braswell, B. H., Schimel, D. S., Linder, E., Moore, B., 1997. The response of global terrestrial ecosystems to interannual temperature variability. Science 278 (5339), 870–872.

Broge, N. H., Leblanc, E., 2001. Comparing prediction power and stability of broadband and hyperspectral vegetation indices for estimation of green leaf area index and canopy chlorophyll density. Remote Sensing of Environment 76 (2), 156–172.

Brosius, F., 2011. SPSS 19. mitp, Heidelberg, Germany.

Busetto, L., Colombo, R., Migliavacca, M., Cremonese, E., Meroni, M., Galvagno, M., Rossini, M., Siniscalco, C., Morra Di Cella, U., Pari, E., 2010. Remote sensing of larch phenological cycle and analysis of relationships with climate in the Alpine region. Global Change Biology 16 (9), 2504–2517.

Chapman, D. S., 2013. Greater phenological sensitivity to temperature on higher Scottish mountains: new insights from remote sensing. Global Change Biology 19 (11), 3463–3471.

Chen, J. M., 1995. Evaluation of vegetation indices and a modified simple ratio for boreal applications. Canadian Journal of Remote Sensing 22 (3), 1–21.

Collins, W., 1978. Remote sensing of crop type and maturity. Photogrammetric Engineering and Remote Sensing 44 (1), 43–55.

Gao, B. C., 1996. NDWI - A normalized difference water index for remote sensing of vegetation liquid water from space. Remote Sensing of Environment 58 (3), 257–266.

Gebhardt, H., Glaser, R., Radtke, U., Reuber, P. (Eds.), 2007. Geographie: Physische Geographie und Humangeographie, 1st Edition. Elsevier, München, Germany.

Guisan, A., Zimmermann, N. E., 2000. Predictive habitat distribution models in ecology. Ecological Modelling 135 (2-3), 147–186.

Haboudane, D., Miller, J. R., Pattey, E., Zarco-Tejada, P. J., Strachan, I. B., 2004. Hyperspectral vegetation indices and novel algorithms for predicting green LAI of crop canopies: Modeling and validation in the context of precision agriculture. Remote Sensing of Environment 90 (3), 337–352.

Halabuk, A., Gerhatova, K., Kohut, F., Ponecova, Z., Mojses, M., 2013. Identification of season-dependent relationships between spectral vegetation indices and aboveground phytomass in alpine grassland by using field spectroscopy. Ekologia 32 (2), 186–196.

Hall, D. K., Riggs, G. A., Salomonson, V. V., 1995. Development of methods for mapping global snow cover using moderate resolution imaging spectroradiometer data. Remote Sensing of Environment 54 (2), 127–140.

Hao, F., Zhang, X., Ouyang, W., Skidmore, A. K., Toxopeus, A. G., 2012. Vegetation NDVI linked to temperature and precipitation in the upper catchments of Yellow River. Environmental Modeling & Assessment 17 (4), 389–398.

Hoye, T. T., Ellebjerg, S. M., Philipp, M., 2007. The impact of climate on flowering in the High Arctic - The case of Dryas in a hybrid zone. Arctic Antarctic and Alpine Research 39 (3), 412–421.

Huete, A., Didan, K., Miura, T., Rodriguez, E., Gao, X., Ferreira, L., 2002. Overview of the radiometric and biophysical performance of the MODIS vegetation indices. Remote Sensing of Environment 83 (1-2), 195–213.

Huete, A. R., 1988. A Soil-Adjusted Vegetation Index (SAVI). Remote Sensing of Environment 25 (3), 295–309.

Huete, A. R., Liu, H. Q., VanLeeuwen, W. J. D., 1997. The use of vegetation indices in forested regions: Issues of linearity and saturation. In: Geoscience and Remote Sensing Symposium (IGARSS). IEEE International, NEW YORK, pp. 1966–1968.

Ide, R., Oguma, H., 2013. A cost-effective monitoring method using digital time-lapse cameras for detecting temporal and spatial variations of snowmelt and vegetation phenology in alpine ecosystems. Ecological Informatics 16, 25–34.

Inouye, D. W., Morales, M. A., Dodge, G. J., 2002. Variation in timing and abundance of flowering by Delphinium barbeyi Huth (Ranunculaceae): the roles of snowpack, frost, and La Nina, in the context of climate change. Oecologica 130 (4), 543–550.

Jehle, M., Hueni, A., Damm, A., D'Odorico, P., Weyermann, J., Kneubühler, M., Schlaepfer, D., Schaepman, M. E., Meuleman, K., 2010. APEX - Current Status, Performance and Validation Concept. In: 2010 IEEE Sensors. 345 E 47TH ST, NEW YORK, NY 10017 USA, pp. 533–537.

Jolly, W. M., Nemani, R., Running, S. W., 2005. A generalized, bioclimatic index to predict foliar phenology in response to climate. Global Change Biology 11 (4), 619–632.

Jordan, C. F., 1969. Derivation of leaf-area index from quality of light on the forest floor. Ecology 50 (4), 663–666.

Kariyeva, J., van Leeuwen, W. J. D., 2011. Environmental drivers of NDVI-based vegetation phenology in Central Asia. Remote Sensing 3 (2), 203–246.

Keshava, N., Mustard, J. F., 2002. Spectral unmixing. IEEE Signal Processing Magazine 19 (1), 44–57.

Kneubühler, M., 2002. Spectral assessment of crop phenology based on spring wheat and winter barley. Remote Sensing Laboratories, Department of Geography University of Zurich, Switzerland.

Kneubühler, M., Damm, A., Schweiger, A., Risch, A. C., Schütz, M., Schaepman, M. E., 2014. Continuous fields from imaging spectrometer data for ecosystem parameter mapping and their potential for animal habitat assessment in alpine regions. IEEE Journal of Selected Topics in Applied Earth Observations and Remote Sensing 7 (6, SI), 2600–2610.

Körner, C., 2007. The use of 'altitude' in ecological research. Trends in Ecology & Evolution 22 (11), 569–574.

Kudo, G., Suzuki, S., 1999. Flowering phenology of alpine plant communities along a gradient of snowment timing. Polar Bioscience 12 (January), 100–113.

Ladinig, U., Wagner, J., 2005. Sexual reproduction of the high mountain plant Saxifraga moschata Wulfen at varying lengths of the growing season. Flora 200 (6), 502–515.

Lausch, A., Salbach, C., Schmidt, A., Doktor, D., Merbach, I., Pause, M., 2015. Deriving phenology of barley with imaging hyperspectral remote sensing. Ecological Modelling 295 (SI), 123–135.

Leuzinger, S., Manusch, C., Bugmann, H., Wolf, A., 2013. A sink-limited growth model improves biomass estimation along boreal and alpine tree lines. Global Ecology and Biogeographie 22 (8), 924–932.

Lieth, H. (Ed.), 1974. Phenology and seasonality modeling. Vol. 8. Springer-Verlag, Berlin.

Lillesand, T. M., Kiefer, R. W., Chipman, J. W., 2008. Remote sensing and image interpretation, 6th Edition. John Wiley & Sons.

Liu, Z., Huang, J., Wu, X., Dong, Y., 2007. Comparison of vegetation indices and red-edge parameters for estimating grassland cover from canopy reflectance data. Journal of Integrative Plant Biology 49 (3), 299–306.

Lu, L., Li, X., Huang, C. L., Ma, M. G., Che, T., Bogaert, J., Veroustraete, F., Dong, Q. H., Ceulemans, R., 2005. Investigating the relationship between ground-measured LAI and vegetation indices in an alpine meadow, north-west China. International Journal of Remote Sensing 26 (20), 4471–4484.

Menzel, A., 2002. Phenology: Its importance to the global change community - An editorial comment. Climatic Change 54 (4), 379–385.

MeteoSchweiz, 2016. IDAWEB Bundesamt für Meteorologie und Klimatologie. Accessed 18.04.2016.
URL `https://gate.meteoswiss.ch/idaweb/login.do`

Mingjun, D., Yili, Z., Linshan, L., Wei, Z., Zhaofeng, W., Wanqi, B., 2007. The relationship between NDVI and precipitation on the Tibetan Plateau. Journal of Geographical Sciences 17 (3), 259–268.

Moser, L., Fonti, P., Büntgen, U., Esper, J., Luterbacher, J., Franzen, J., Frank, D., 2010. Timing and duration of European larch growing season along altitudinal gradients in the Swiss Alps. Tree Physiology 30 (2), 225–233.

Mutanga, O., Skidmore, A. K., 2004. Narrow band vegetation indices overcome the saturation problem in biomass estimation. International Journal of Remote Sensing 25 (19), 3999–4014.

Nemani, R. R., Keeling, C. D., Hashimoto, H., Jolly, W. M., Piper, S. C., Tucker, C. J., Myneni, R. B., Running, S. W., 2003. Climate-driven increases in global terrestrial net primary production from 1982 to 1999. Science 300 (5625), 1560–1563.

Nichol, J., Wong, M. S., 2007. Remote sensing of urban vegetation life form by spectral mixture analysis of high-resolution IKONOS satellite images. International Journal of Remote Sensing 28 (5), 985–1000.

Psomas, A., Kneubuehler, M., Huber, S., Itten, K., Zimmermann, N. E., Kneubühler, M., Huber, S., Itten, K., Zimmermann, N. E., 2011. Hyperspectral remote sensing for estimating aboveground biomass and for exploring species richness patterns of grassland habitats. International Journal of Remote Sensing 32 (24), 9007–9031.

Qi, J., Chehbouni, A., Huete, A. R., Kerr, Y. H., Sorooshian, S., 1994. A modified soil adjusted vegetation index. Remote Sensing of Environment 48 (2), 119–126.

Ren, H., Feng, G., 2014. Are soil-adjusted vegetation indices better than soil-unadjusted vegetation indices for above-ground green biomass estimation in arid and semi-arid grasslands? Grass and Forage Science 70 (4), 611–619.

Richardson, A. D., Keenan, T. F., Migliavacca, M., Ryu, Y., Sonnentag, O., Toomey, M., 2013. Climate change, phenology, and phenological control of vegetation feedbacks to the climate system. Agricultural and Forest Meteorology 169, 156–173.

Richter, R., Schläpfer, D., 2002. Geo-atmospheric processing of airborne imaging spectrometry data. Part 2:Atmospheric/topographic correction. International Journal of Remote Sensing 23 (13), 2609–2630.

Risch, A. C., Jurgensen, M. F., Page-Dumroese, D. S., Wildi, O., Schütz, M., 2008. Long-term development of above- and below-ground carbon stocks following land-use change in subalpine ecosystems of the Swiss National Park. Canadien Journal of Forest Research 38 (6), 1590–1602.

Rouse, J. W., Haas, R. H., Schell, J. A., Deering, D., 1974. Monitoring vegetation systems in the Great Plains with ERTS". In: Proceedings, Third Earth Resources Technology Satellite-1 Symposium. Vol. 1. NASA GSFC, Greenbelt, MD. SP-351„ pp. 309–317.

Rundquist, B. C., 2002. The influence of canopy green vegetation fraction on spectral measurements over native tallgrass prairie. Remote Sensing of Environment 81 (1), 129–135.

Schaepman, M. E., Jehle, M., Hueni, A., D'Odorico, P., Damm, A., Weyerrnann, J., Schneider, F. D., Laurent, V., Popp, C., Seidel, F. C., Lenhard, K., Gege, P., Küchler, C., Brazile, J., Kohler, P., De Vos, L., Meuleman, K., Meynart, R., Schlaepfer, D., Kneubühler, M., Itten, K. I., 2015. Advanced radiometry measurements and Earth science applications with the Airborne Prism EXperiment (APEX). Remote Sensing of Environment 158, 207–219.

Schläpfer, D., Richter, R., 2002. Geo-atmospheric processing of airborne imaging spectrometry data. Part 1: Parametric orthorectification. International Journal of Remote Sensing 23 (13), 2609–2630.

Schmid, C., 2016. Atlas des Schweizerischen Nationalparks: Die Erweiterung. Accessed 18.04.2016.
URL `http://www.atlasnationalpark.ch/node/393`

Schultz, P. A., Halpert, M. S., 1993. Global correlation of temperature, NDVI and precipitation. Advances in Space Research 13 (5), 277–280.

Schütz, M., Risch, A. C., Leuzinger, E., Krüsi, B. O., Achermann, G., 2003. Impact of herbivory by red deer (Cervus elaphus L.) on patterns and processes in subalpine grasslands in the Swiss National Park. Forest Ecology and Management 181 (1-2), 177–188.

Shen, M., Tang, Y., Klein, J., Zhang, P., Gu, S., Shimono, A., Chen, J., 2008. Estimation of aboveground biomass using in situ hyperspectral measurements in five major grassland ecosystems on the Tibetan Plateau. Journal of Plant Ecology 1 (4), 247–257.

Smith, A. M. S., Lentile, L. B., Hudak, A. T., Morgan, P., 2007. Evaluation of linear spectral unmixing and DNBR for predicting postfire recovery in a North American ponderosa pine forest. International Journal of Remote Sensing 28 (22), 5159–5166.

Sun, J., Cheng, G., Li, W., Sha, Y., Yang, Y., 2013. On the variation of NDVI with the principal climatic elements in the Tibetan Plateau. Remote Sensing 5 (4), 1894–1911.

Szeicz, G., 1974. Solar-radiation for plant growth. Journal of Applied Ecology 11 (2), 617–636.

Theurillat, J. P., Guisan, A., 2001. Potential impact of climate change on vegetation in the European Alps: A review. Climatic Change 50 (1-2), 77–109.

Totland, O., 1997. Effects of flowering time and temperature on growth and reproduction in Leontodon autumnalis var. taraxaci a late-flowering alpine plant. Arctic and Alpine Research 29 (3), 285–290.

Verrelst, J., Schaepman, M. E., Koetz, B., Kneubühler, M., 2008. Angular sensitivity analysis of vegetation indices derived from CHRIS/PROBA data. Remote Sensing of Environment 112 (5), 2341–2353.

Vescovo, L., Gianelle, D., 2008. Using the MIR bands in vegetation indices for the estimation of grassland biophysical parameters from satellite remote sensing in the Alps region of Trentino (Italy). Advances in Space Research 41 (11), 1764–1772.

Wang, J., Rich, P. M., Price, K. P., 2003. Temporal responses of NDVI to precipitation and temperature in the central Great Plains, USA. International Journal of Remote Sensing 24 (11), 2345–2364.

Wang, Y., Hou, X., Wang, M., Wu, L., Ying, L., Feng, Y., 2013. Topographic controls on vegetation index in a hilly landscape: A case study in the Jiaodong Peninsula, eastern China. Environmental Earth Sciences 70 (2), 625–634.

White, K., Pontius, J., Schaberg, P., 2014. Remote sensing of spring phenology in northeastern forests: A comparison of methods, field metrics and sources of uncertainty. Remote Sensing of Environment 148, 97–107.

White, M. A., de Beurs, K. M., Didan, K., Inouye, D. W., Richardson, A. D., Jensen, O. P., O'Keefe, J., Zhang, G., Nemani, R. R., van Leeuwen, W. J. D., Brown, J. F., de Wit, A., Schaepman, M., Lin, X., Dettinger, M., Bailey, A. S., Kimball, J., Schwartz, M. D., Baldocchi, D. D., Lee, J. T., Lauenroth, W. K., 2009. Intercomparison, interpretation, and assessment of spring phenology in North America estimated from remote sensing for 1982-2006. Global Change Biology 15 (10), 2335–2359.

White, M. A., Nemani, R. R., 2006. Real-time monitoring and short-term forecasting of land surface phenology. Remote Sensing of Environment 104 (1), 43–49.

Whittaker, R. H., Niering, W. A., 1975. Vegetation of the Santa Catalina Mountains, Arizona. V. Biomass, production, and diversity along the elevation gradient. Ecology 56 (4), 771–790.

Wipf, S., Rixen, C., Mulder, C. P. H., 2006. Advanced snowmelt causes shift towards positive neighbour interactions in a subarctic tundra community. Global Change Biology 12 (8), 1496–1506.

Yang, W., Yang, L., Merchant, J. W., 1997. An assessment of AVHRR/NDVI-ecoclimatological relations in Nebraska, USA. International Journal of Remote Sensing 18 (10), 2161–2180.

Yang, X., Guo, X., Fitzsimmons, M., 2012. Assessing light to moderate grazing effects on grassland production using satellite imagery. International Journal of Remote Sensing 33 (16), 5087–5104.

Zhang, L., Furumi, S., Muramatsu, K., Fujiwara, N., Daigo, M., Zhang, L., 2007. A new vegetation index based on the universal pattern decomposition method. International Journal of Remote Sensing 28 (1-2), 107–124.

Ziello, C., Estrella, N., Kostova, M., Koch, E., Menzel, A., 2009. Influence of altitude on phenology of selected plant species in the Alpine region (1971-2000). Climate Research 39 (3), 227–234.

Nomenclature

aAF averaged All Forest

aAG averaged All Grassland

aFNE averaged Forest Noth-East

aFSW averaged Forest South-West

AG All Grassland

aGNE averaged Grassland North-East

aGSW averaged Grassland South-West

aL50 averaged Larch 50

aL60 averaged Larch 60

aL70 averaged Larch 70

aL92 averaged Larch 92

APEX IS Airborne Prism EXperiment Imaging Spectrometer

CO2 Carbon dioxid

DEM Digital Elevation Model

DOY Day Of Year

FNE Forest North-East

fNIR far Near InfraRed

FSW Forest South-West

GD Growing Days between SOPS and DOY 175

GDD Growing Degree Days

GDD0 Growing Degree Days with temperature above 0°C

GDD5 Growing Degree Days with temperature above 5°C

GNE Grassland North-East

GR Global Radiation

GSW	Grassland South-West
L50	Larch 50
L60	Larch 60
L70	Larch 70
L92	Larch 92
LAI	Leaf Area Index
LSU	Linear Spectal Unmixing
MIR	Middle InfraRed
MSAVI2	Modified Soil Adjusted Vegetation Index 2
NCI	Normalized Canopy Index
NDSI	Normalized Differenced Snow Index
NDVI	Normalized Differential Vegetation Index
NDWI	Normalized Difference Water Index
NIR	Near InfraRed
nNIR	near Near InfraRed
O2	Oxygen
PD	Days with Precipitation
pH	Potential of Hydrogen
PT	Total amount of Precipitation
RS	Remote Sensing
SAVI	Soil Adjusted Vegetation Index
SD	Sunshine Duration
SNP	Swiss National Park
SOPS	Start Of Phenological Season
SR	Simple Ratio
SWIR	Short Wave InfraRed
T	Temperature
TM	Landsat Thematic Mapper

VI	Vegetation Index
VIS	Visible Spectrum
VNIR	Visible/ Near InfraRed

A. Additional Results

A.1. Kolmogorov-Smirnov Distribution

A.2. Correlation Coefficient

Table A.1.: Kolmogorov-Smirnov distribution with significant α (http://www.statistik.tuwien.ac.at/public/dutt/vorles/mb_wi_vt/node98.html).

	α				
n	0.1	0.05	0.025	0.01	0.005
1	.9000	.9500	.9750	.9900	.9950
2	.6838	.7764	.8419	.9000	.9293
3	.5648	.6360	.7076	.7846	.8290
4	.4927	.5652	.6239	.6889	.7342
5	.4470	.5094	.5633	.6272	.6685
6	.4104	.4680	.5193	.5774	.6166
7	.3815	.4361	.4834	.5384	.5758
8	.3583	.4096	.4543	.5065	.5418
9	.3391	.3875	.4300	.4796	.5133
10	.3226	.3687	.4092	.4566	.4889
11	.3083	.3524	.3912	.4367	.4677
12	.2958	.3382	.3754	.4192	.4490
13	.2847	.3255	.3614	.4036	.4325
14	.2748	.3142	.3489	.3897	.4176
15	.2659	.3040	.3376	.3771	.4042
16	.2578	.2947	.3273	.3657	.3920
17	.2504	.2863	.3180	.3553	.3809
18	.2436	.2785	.3094	.3457	.3706
19	.2373	.2714	.3014	.3369	.3612
20	.2316	.2647	.2941	.3287	.3524
21	.2262	.2586	.2872	.3210	.3443
22	.2212	.2528	.2809	.3139	.3367
23	.2165	.2475	.2749	.3073	.3295
24	.2120	.2424	.2693	.3010	.3229
25	.2079	.2377	.2640	.2952	.3166
26	.2040	.2332	.2591	.2896	.3106
27	.2003	.2290	.2544	.2844	.3050
28	.1968	.2250	.2499	.2794	.2997
29	.1935	.2212	.2457	.2747	.2947
30	.1903	.2176	.2417	.2702	.2899
31	.1873	.2141	.2379	.2660	.2853
32	.1844	.2108	.2342	.2619	.2809
33	.1817	.2077	.2308	.2580	.2768
34	.1791	.2047	.2274	.2543	.2728
35	.1766	.2018	.2242	.2507	.2690
36	.1742	.1991	.2212	.2473	.2653
37	.1719	.1965	.2183	.2440	.2618
38	.1697	.1939	.2154	.2409	.2584
39	.1675	.1915	.2127	.2379	.2552
40	.1655	.1891	.2101	.2349	.2521
Approximation für $n > 40$	$\frac{1.07}{\sqrt{n}}$	$\frac{1.22}{\sqrt{n}}$	$\frac{1.36}{\sqrt{n}}$	$\frac{1.52}{\sqrt{n}}$	$\frac{1.63}{\sqrt{n}}$

Table A.2.: Correlation coefficient definition by Brosius (2011).

correlation coefficient	Possible interpretation
0	No correlation
Over 0 to 0.2	Very week correlation
0.2 to 0.4	Week correlation
0.4 to 0.6	Mean correlation
0.6 to 0.8	Strong correlation
0.8 to nearly 1	Very strong correlation
1	Perfect correlation

B. Personal Declaration

I hereby declare that the submitted thesis is the result of my own, independent work. All external sources are explicitly acknowledged in the thesis.

Seuzach, 29.04.2016